Balancing the force budget of plate tectonics along the Nazca/South America plate margin

Dissertation der Fakultät für Geowissenschaften der
Ludwig-Maximilians Universität München

Vorgelegt von
Giampiero Iaffaldano
am 10.09.2007

Erstgutachter: Prof. Dr. Hans-Peter Bunge

Zweitgutachter: Prof. Dr. Stuart Gilder

Tag der mündlichen Prüfung: 06/12/2007

Table of contents

Introduction

Understanding the dynamics of global plate motion is one of the most important problems in geophysics today. Mantle convection is commonly accepted as the driving force for plates but, while the kinematics of plate movement is well known from geodetic and paleomagnetic observations, we still lack a rigorous description of the coupled mantle convection-plate motion system.

Over the past 10 years there has been much progress in developing and exploring computational high-resolution 3D mantle convection models. These geodynamic earth models solve the conservation equations (mass, momentum, energy) for a highly viscous (Stokes) fluid. The use of local finite elements in some of these models allows one furthermore to make use of modern parallel computers. In particular the advance of cost-efficient networked PCs, so called Beowulf clusters, has enabled researchers to achieve sufficient spatial resolution (typically more than 100 million grid points are used in geodynamic model calculations today) to fully resolve the dynamically important length scales (thermal boundary layers) of convective motion in the Earth's mantle. While these advances in mantle convection modeling are encouraging, the main shortcoming of geodynamic models today is their lack of a realistic treatment of

the lithosphere, and in particular of the lack of faults which arise from the brittle nature of rock failure in the uppermost cold regions of plates.

Independently of advances in mantle convection models, there has been a substantial progress in the development of global lithospheric models. Based on stress-equilibrium and sophisticated non-linear material flow laws these models include finite element formulations that account explicitly for surface topography, lithosphere structure and thickness and geological faults through the use, for example, of contact elements. In the past these models have been used to compute global plate velocities and stress distributions from parameterized shear tractions at the base of the lithosphere.

The logical step to take then is to merge together these two classes of numerical models in order to gain a comprehensive description of the whole convecting system. Over the past four years I focused on coupling two of these numerical such that I'm in possession now of a dynamically consistent model for lithosphere and mantle dynamics, where forces driving plates account for shear tractions from the mantle exerted at the base of plates and tectonic stresses originated by regional variations in lithosphere structure and topography.

The global mantle convection code I'm using is TERRA developed by Dr. Baumgardner (Los Alamos National Laboratory) and Prof. Bunge (at the Ludwig

Maximilians University of Munich). The code is based on an icosahedral grid of finite elements and an efficient multigrid algorithm to solve the elliptic problem arising from the momentum equation. The code is fully parallelized and performs well on PC-Beowulf clusters.

The lithosphere motion code I use is SHELLS developed by Prof. Bird (UCLA, California), based on 2D (thin shell) triangular global grid it is capable to provide surface velocity and stress maps.

I use a global mantle convection model [Bunge et al., 1997] in conjunction with a global model of the lithosphere [Kong and Bird, 1995] to compute plate motions consistent with shear tractions arising from realistic mantle convection calculations. The 3-D spherical mantle convection model solves the conservation equations of mass (a), momentum (b) and energy (c) for a highly viscous (Stokes) fluid in order to compute temperature and velocity throughout the mantle.

a) $\quad div(\bar{v}) = 0$

b) $\quad -\nabla p + \mu \nabla^2 \bar{v} - \rho g \hat{e}_r = 0$

c) $\quad \dfrac{\partial T}{\partial t} = -v \nabla T + k \nabla^2 T + H$

In the above equations v = velocity, p = pressure, μ = viscosity, ρ = density, g =

gravitational acceleration, T = temperature, t = time, k = thermal conductivity and H = radiogenic heat production rate. A multi-grid technique is used to solve the elliptic problem arising from the Stokes flow in a highly efficient manner. The use of local finite elements allows us furthermore to take advantage of modern parallel computers so that high numerical resolution can be achieved sufficient to resolve the dynamically important length-scales (thermal boundary layers) of convective motion in the Earth's mantle. Mantle buoyancy forces are derived from a history of plate motion and subduction that spans the past 120 m.y. [Lithgow-Bertelloni and Richards, 1998]. The lithosphere model (SHELLS) is based on conservation of momentum (stress equilibrium) and uses non-linear material flow laws. In order to compute plate velocities, the code solves for the momentum (d) and mass (see above) conservation equations

d) $-\rho g \hat{e}_r + \dfrac{\partial \sigma_{ij}}{\partial x_j} = 0$

in the thin-sheet approximation [Bird, 1999], where the 3-D force balance is vertically integrated along depth in order to reduce the 3-D problem to 2-D. In the above equation ρ = density, g = gravitational acceleration and σ = stress. The lithosphere model uses finite elements with a computational grid that accounts explicitly for geological faults by means of interfaces between contact elements (Fig. I.1). At each

node of the computational grid, the stresses involved in the dynamics of the lithosphere include the ones coming from large topography regions on the surface of the upper plate (which contribute both through horizontal deviatoric stresses and vertical overburden pressure), and the shear stresses from the mantle. No vertical shear traction is assumed on vertical planes so that vertical normal stresses are lithostatic at all nodes, and equal to the weight of the overburden per unit area. In the quasi steady state of the lithospheric force balance considered in the formulation, elasticity contributes a negligible fraction of the strain rate in viscoelastic solutions. Elastic strain is then entirely neglected to eliminate arbitrary initial conditions and time-steps. Temperature plays an important role in defining the rheological properties of the deep crust and lithosphere; in SHELLS thermal conductivity and heat productivity are assumed to be constant laterally. Moreover the vertical heat conduction is assumed to be steady state. Faults and plate boundaries are represented in the computational grid through contact elements. The fault dip angle is allowed to vary laterally and is constrained directly from seismological observations. The rheological properties at faults differ from the ones of continuum (intraplate) elements and are such that faults are weaker with respect to non-faulted material. Specifically at each fault three rheologic laws are evaluated: frictional (Mohr-Coulomb) faulting, dislocation and Newtonian creep. At each depth along the fault plane and depending on temperature, pressure and strain rate, the mechanism giving the lowest shear stress is the one

presumed to dominate. As for the frictional regime, the tectonic model (Shells) accounts for a fault friction value equal to 0.03, much lower than suggested by Byerlee's low for non faulted material (0.85), and in agreement with a number of observations suggesting low fault friction coefficients, including heatflow measurements and stress directions in transform faults. Concerning the dislocation creep regime (e), stress (σ) is proportional to strain rate (ε)

e) $$\sigma = A \cdot \left(\dot{\varepsilon} \right)^{1/n} \cdot \exp\left[\frac{B + Cz}{T} \right]$$

Where σ = stress, $\dot{\varepsilon}$ = strain rate and T = temperature at depth z. I use the following values for crust and mantle layers: A (Pa*s**1/n) = 3.2*10**7 (crust) / 3.4*10**4 (lithosphere), B (activation energy in ° K) = 10048 (crust) / 21340 (lithosphere), C (° K*m**-1) = 0 (crust) / 0.0223 (lithosphere) and n = 3 (both crust and lithosphere). Once all the stresses have been computed, SHELLS determines plate velocities that equilibrate those stresses. The link between the mantle and lithosphere model is performed by using the asthenosphere velocities derived from the MCMs as a velocity boundary condition at the base of plates in SHELLS, such that realistic mantle buoyancy forces are allowed to drive plate motion. Plate driving tractions are computed in SHELLS through a dislocation olivine creep rheology that depends on

temperature, pressure and strain rate, where the strain rate is equal to the vertical gradient of the asthenosphere velocity pattern from MCMs.

With the aid of such joint numerical models and by exploiting the enormous amount of plate motions data available today through both paleomagnetic and geodetic techniques, I direct my research toward a better understanding of plate boundary tectonic forces, how do they change in time and how do they compare to other driving forces in plate tectonics. It is in fact only with the advent over the last decade or so of highly precise geodetic measurements that we have gained a perspective of how plates move today. Armed with the new techniques, especially the Global Positioning System (GPS), we are now in a position to measure present-day plate motions at unprecedented precision and compare them to their motion in the past inferred from paleomagnetic observations. The ability to consider past as well as present plate motions is an incredible source of information to understand the dynamics of lithosphere. The principle of inertia tells us that a change in plate motion must necessarily be related to a change in one or more forces acting upon plates. Unfortunately the geologic experiments performed for us by nature are neither repeatable nor controllable, so we must build sophisticated computer models and try to reproduce into a computer observed plate motions and motion changes over time in order to test hypotheses and to clearly understand the dynamics of how plates move.

References

Bird, P., 1999, SHELLS: Thin-plate and thin-shell finite element programs for forward dynamic modeling of plate deformation and faulting: Computers & Geosciences, v. 25, p. 383-394.

Bunge, H.-P., Richards, M. A., Baumgardner, J. R., 1997, A sensitivity study of 3-D spherical mantle convection at 10exp8 Rayleigh number: Effects of depth dependent viscosity, heating mode and an endothermic phase change: Journal of Geophysical Research, v. 102, p. 11,991 - 12,007.

Kong, X., Bird, P., 1995, SHELLS: A thin-shell program for modeling neotectonics of regional or global lithosphere with faults: Journal of Geophysical Research, v. 100, p. 22,129-22,132.

Lithgow-Bertelloni, C., Richards, M. A., 1998, The Dynamics of Cenozoic and Mesozoic Plate Motions: Review of Geophysics, v. 36, p. 27-78.
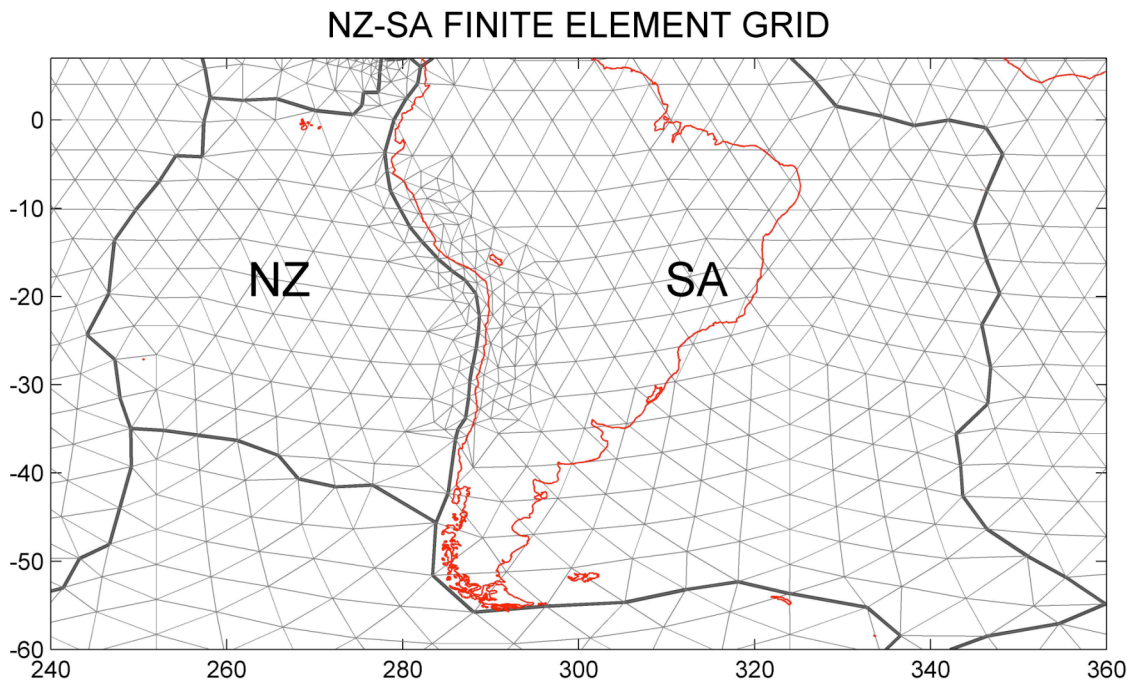
Fig. I.1. Global finite element grid focused on the Nazca/South America region. Triangular elements are in gray, plate boundaries in bold gray, coastline in red.

Chapter 1

Feedback between mountain belt growth and plate convergence

SUMMARY

While it is generally assumed that global plate motions are driven by the pattern of convection in the Earth's mantle, the details of that link remain obscure. Buoyancy forces associated with subduction of cool, dense lithosphere at zones of plate convergence are thought to provide significant driving force, but the relative magnitudes of other driving and resisting forces are less clear, as are the main factors controlling long-term changes in plate motion. The ability to consider past as well as present plate motions provides significant additional constraints, because changes in plate motion are necessarily driven by changes in one or more driving or resisting forces, which may be inferred from independent data. Here we present for the first time a model that explicitly links global mantle convection and lithosphere models to infer plate motion changes as far back as

Miocene time. By accurately predicting observed convergence rates over the past 10 m.y., we demonstrate that surface topography generated at convergent margins is a key factor controlling the long-term evolution of plate motion. Specifically, the topographic load of large mountain belts and plateaus consumes a significant amount of the driving force available for plate tectonics by increasing frictional forces between downgoing and overriding plates.

INTRODUCTION

A central tenet of plate tectonics states that Earth's surface moves as rigid units, while most of the deformation occurs along plate margins [Morgan, 1968]. At converging boundaries the deformation often generates large topography. Two prominent examples are the Tibet and Andes regions, where stress accumulation at the adjacent subduction zones produces lithospheric shortening and consequent uplift of high mountain plateaus in a process that in both cases is still active today [Molnar et al., 1993; Allmendinger et al., 1997]. Less certain is whether the resulting topography (4 - 5 km) in turn affects plate convergence and the dynamics of how plates move. There are important constraints on the dynamics of plate motion from the record of past plate velocities. Geologic plate reconstructions [Gordon and Jurdy, 1986; Lithgow-

Bertelloni and Richards, 1998] reveal significant temporal variations in plate velocities for the Cenozoic period. These observations are augmented by a growing body of space geodetic data capable of mapping present-day plate velocities with unprecedented accuracy. For example, the Global Positioning System (GPS) measures relative plate velocities to a precision of a few millimeters/year or better [Dixon, 1991; Gordon and Stein, 1992]. In general, present plate motions are remarkably similar to models averaged over the past few million years such as NUVEL-1A [DeMets et al., 1994; Sella et al., 2002]; however, the Nazca and South America plates are important exceptions. By comparing geodetic data with plate velocities predicted from NUVEL-1A, Norabuena et al. [1998] observed that present rates of Nazca–South America convergence are slower than their 3.2 m.y. average. The geodetic measurements constrain present-day relative motion between the Nazca and South America plates; at a point on the plate boundary, long 71.5°W, lat 25°S (all convergence rates herein are computed at this location), we obtain a convergence rate of 6.7 ± 0.2 cm/yr using the angular velocity vector of Sella et al. [2002]; reconstructions of Gordon and Jurdy [1986] indicate a 10.3 ± 0.2 cm/yr convergence averaged over the past 10 m.y. (Figs. 1.1a and 1.1b). The velocity reduction is also confirmed by long-term (40 m.y.) reconstructions of Nazca (Farallon)–South America plate motion [Somoza, 1998]. The most significant tectonic change in the region for the past 25 m.y. is the growth of the high Andes along the western margin of South America, in particular the rise of the

Altiplano and Puna plateaus 10 m.y. ago. Norabuena et al. [1999] suggested that Nazca–South America convergence slowed in response to Miocene–Pliocene uplift of the Andes, because the gravitational load of the mountain belt might increase the stress level on the dipping plate boundary. The tectonic plates comprise the cold upper thermal boundary layer of mantle convection [Davies, 1999]. In recent years there has been great progress in our ability to simulate three-dimensional (3-D) spherical mantle convection at high numerical resolution [Tackley et al., 1994; Bunge et al., 1997; Zhong et al., 2000]. Combined with constraints on the history of subduction [Richards and Engebretson, 1992] one can exploit the computer simulations to construct mantle circulation models (MCMs) [Bunge et al., 1998]. These time-dependent earth models map temporal variations of large-scale mantle flow. MCMs thus allow us to place first-order estimates on the internal mantle buoyancy forces that drive plate motion. There have been great advances in the development of sophisticated global models of the lithosphere independent of the MCM development. One approach employs isostasy and vertical integration of lithospheric strength to reduce the 3-D problem to two dimensions in what is known as thin-shell tectonic modeling. Here we apply one such model [SHELLS; Kong and Bird, 1995] that includes driving forces from topography, a temperature-dependent viscous rheology, and faults at plate boundaries. Although the code reduces the geometry from 3-D to 2-D, it provides a realistic representation of the strength of rocks that accommodate Coulomb frictional sliding along faults in the

15

cold upper brittle portion of the lithosphere and dislocation creep in the warm deeper ductile regions of the plates. Faults are implemented by means of finite-element interfaces where the fault dip angle is determined from seismological observations. We use the lithospheric model in conjunction with present-day plate driving forces from the MCM to explore the impact of high Andean topography on the velocity of the Nazca plate (details about methods are given in Appendix A). In our approach, the asthenosphere velocities computed from the MCM are applied as boundary conditions at the base of plates in SHELLS. Plate driving tractions are then computed in SHELLS. The MCM parameters were described by Bunge et al. [2002]; they account for radial variations in mantle viscosity (factor 40 increase from the upper to the lower mantle), internal heat generation from radioactivity, bottom heating from the core, and a history of subduction spanning the past 120 m.y.

MODEL AND RESULTS

We compute global plate velocities with SHELLS assuming mantle shear tractions from the MCM and a fault friction coefficient of 0.03. This fault friction value is supported by experimental evidence [Hickman, 1991] and is consistent with a range of independent numerical modeling results [Hassani et al., 1997; Bird, 1998; Sobolev and

16

Babeyko, 2005]. To clearly isolate the effect of Andean topography, we perform two global plate motion simulations. First, our input topography is the one reported in the ETOPO5 data set [National Geophysical Data Center, 1998] with the Andes reaching an altitude of 4 km (Fig. 1.2b). This simulation is meant to represent present-day plate motions. We perform a second simulation with ETOPO5 elevation everywhere except for the Andes, where we use an estimate of paleotopography from published data [Gregory Wodzicki, 2000; Lamb and Davies, 2003] based on a range of botanic and geologic indicators (Fig. 1.2a). Plate velocities computed in this second scenario are meant to represent conditions at 10 m.y. ago. To keep the modeling assumptions simple, mantle buoyancy forces are equal in both simulations. MCM modeling suggests that large scale mantle heterogeneity evolves on a time scale of 50–100 m.y., comparable to a mantle overturn time and substantially larger than the 10 m.y. time period considered here. We also keep global plate geometry constant consistent with the reconstructions of Gordon and Jurdy [1986], who cast the global plate geometry of the past 10 m.y. into a single stage. Fig. 1.2 shows the computed Nazca plate velocity for the two cases in the South American reference frame. The case with topography corresponding to presumed conditions at 10 m.y. ago (Fig. 1.2a) results in a convergence of 10.1 cm/yr while the case corresponding to present Andean topography results in a 6.9 cm/yr plate convergence (Fig. 1.2b). These two values are in excellent agreement with the inferences, respectively, by Gordon and Jurdy [1986]

(Fig. 1.1a) for Nazca–South America plate motion over the past 10 m.y. and with the geodetic constraints for present-day convergence (Fig. 1.1b). The computed Euler vectors from the two simulations agree with the observed rotation poles at the 68% confidence level in both position and rotation rate. Could it be coincidence that the deceleration of the Nazca plate over the past 10 m.y. correlates with the assumed Andean uplift history? We address this question by considering two additional constraints to bear on our calculations. First, there is a large body of evidence to suggest that a significant portion of the current elevation of the Altiplano-Puna plateau was achieved prior to the past 5 m.y. Support for this comes from recent paleomagnetic work in the Peruvian Cordillera that demonstrates that rapid deformation and counterclockwise rotation occurred in geologic strata older than 9 Ma, while there is no evidence for such rotation in strata younger than 7 Ma [Rousse et al., 2002]. Support comes from paleoaltimetry studies based on measurements of the abundances of 13C-18O bonds in soil carbonates that suggest that most of the Altiplano uplift took place between 10.3 and 6.7 m.y. ago [Ghosh et al., 2006]. The tectonic deformation age is thus between 10 and 7 Ma. Second, there is further temporal information for relative Nazca–South America plate motion available from NUVEL-1A. De Mets et al. [1994] estimated the average Nazca–South America convergence at 8.0 ± 0.2 cm/yr for the past 3.2 m.y., less than the 10.3 ± 0.2 cm/yr value inferred by Gordon and Jurdy [1986] for the past 10 m.y., but still higher than

the geodetic measure of current plate convergence (6.7 ± 0.2 cm/yr) from Norabuena et al. [1999]. Thus it appears that the most rapid deceleration of the Nazca plate occurred during the period of the most pronounced Andean uplift. We test this notion explicitly in a third simulation. In accord with estimates for Andean paleotopography ~3 m.y. ago we assume a 3 km elevation for the central Andes (Fig. 1.3a) and find that this scenario results in a Nazca–South America convergence of 7.9 cm/yr (Fig. 1.3b). Note that this value is in excellent agreement with the NUVEL-1A model. Our results beg an important question. Do large mountain belts like the Andes generate resistive fault stresses that are comparable to the driving forces of plate tectonics? We address this question in Fig. 1.4, where we plot fault stresses and mantle shear tractions from our simulation for the present day beneath the Nazca and South America plates. Beneath the mountain belt, the subduction plane undergoes frictional stresses as high as 5 MPa, especially under highly elevated regions such as the Puna and Altiplano plateaus. These resistive stresses are comparable to the mantle shear tractions in our model. In our global plate tectonic simulations it is logical to ask whether the effect of mountain belts is spatially confined to the plates sharing the convergent margin. We address this question in Fig. 1.5a. Here we simultaneously plot the two sets of velocity directions corresponding, respectively, to our case with assumed conditions of Andean topography 10 m.y. ago and to our case with today's topography, both in the hotspot reference frame. We also show the absolute scalar magnitude of the velocity

difference. Although there are some modest velocity differences, primarily for the African, North American, and Eurasian plates, the most important effect on plate motion from Andean uplift is focused at the velocity of the Nazca and South America plates. Fig. 1.5b is identical to Fig. 1.5a, except that our calculation corresponding to conditions 10 m.y. ago accounts for the inferred uplift of Tibet, which we model here in addition to the Andean uplift. A range of data supports a significant uplift of Tibet starting between 13 and 9 m.y. ago, coeval with age estimations for the major uplift phase in South America. In this case the velocity differences for the Nazca plate and South America (2 cm/yr) are the same that we found before, plus relatively smaller velocity differences, up to 0.6 cm/yr, in the Australian and the Eurasian plate. Thus the presumed growth of Tibet does not significantly alter our inference on Nazca–South America convergence, as expected from our results in Fig. 1.5a.

DISCUSSION

Our modeling results are of great interest because an increasing number of plate kinematic constraints are now available on the temporal variations of how plates move. While there has been substantial but separate progress in the development of MCMs and tectonic models of the lithosphere, our simulations suggest that these models are

beginning to achieve a level of maturity such that their joint application may prove useful to exploit these constraints and to test some first order hypotheses on the dynamics of plate motion. The strong influence of mountain belts on the velocity of plates may seem unexpected. We verified that the overburden pressure associated with 4 km relief in the high Andes raises the frictional forces along the main plate bounding fault plane by $\sim 1*10**13$ N/m, a value that is significant compared to other key forces in plate tectonics. Recent 2-D geodynamic modeling [Husson and Ricard, 2004] of the Andean orogeny shows that the total transmitted force between subducting and overriding plate is $\sim 9*10**12$ N/m. This value is consistent with our calculations and is supported by observations of large negative gravity variations along the Nazca–South America trench [Song and Simons, 2003]. More important, the magnitude of frictional fault stresses is comparable to shear stresses in the mantle and implies that the topographic load of large mountain plateaus may consume a significant amount of the driving forces available for plate tectonics. The latter observation may have profound implications. Raymo and Ruddiman [1992] suggested that Cenozoic climate change may have been caused by the uplift of Tibet; i.e., the rise of large mountain plateaus may affect climate. Lamb and Davis [2003] speculated that the reverse may be true for the Andes. Because these mountains act as an orographic barrier against moisture-bearing winds, they result in regional aridity and reduced erosion. Low erosion rates, however, have been implicated as a prerequisite for the creation of large

plateaus such as the Altiplano [Sobel et al., 2003]; i.e., climate may act as a force on plate tectonics. We emphasize the large uncertainties associated with estimates of the Andean paleotopography. While our results are intriguing, a more robust relation between Andean topography and the velocity of the Nazca plate awaits improved constraints on the elevation history of the Andes.

REFERENCES

Allmendinger, R. W., Jordan, T. E., Kay, S. M., Isacks, B. L., 1997, The evolution of the Altiplano-Puna plateau of the central Andes: Annual Review of Earth and Planetary Sciences, v. 25, p. 139-174.

Bird, P., 1998, Testing hypotheses on plate-driving mechanisms with global lithosphere models including topography, thermal structure, and faults: Journal of Geophysical Research, v. 103, p. 10,115-10,129.

Bunge, H.-P., Richards, M. A., Baumgardner, J. R., 1997, A sensitivity study of 3-D spherical mantle convection at 10**8 Rayleigh number: Effects of depth dependent viscosity, heating mode and an endothermic phase change: Journal of Geophysical Research, v. 102, p. 11,991-12,007.

Bunge, H.-P., Richards, M. A., Lithgow-Bertelloni, C., Baumgardner, J. R., Grand, S. P., Romanowicz, B. A., 1998, Time scales and heterogeneous structure in geodynamic earth models: Science, v. 280, p. 91-95.

Bunge, H.-P., Richards, M. A., Baumgardner, J. R., 2002, Mantle-circulation models with sequential data assimilation: inferring present-day mantle structure from plate-motion histories: Philosophical Transactions of the Royal Society of London Ser. A, v. 360, p. 2545-2567.

Davies, G. F., 1999, Dynamic Earth: Cambridge, Cambridge University Press, 455 p.

DeMets, C., Gordon, R. G., Argus, D. F., Stein, S., 1994, Effect of recent revisions to the geomagnetic reversal time scale on estimates of current plate motions: Geophysical Research Letters, v. 21, 2191-2194.

Dixon, T. H., 1991, An introduction to the Global Positioning System and some geological applications: Reviews of Geophysics, v. 29, p. 249-276.

Ghosh, P., Garzione, C. N., Eiler, J. M., 2006, Rapid Uplift of the Altiplano Revealed Through 13C-18O Bonds in Paleosol Carbonates: Science, v. 311, p. 511-515.

Gordon, R. G., Jurdy, D. M., 1986, Cenozoic global plate motions: Journal of Geophysical Research, v. 91, p. 12,389-12,406.

Gordon, R. G., Stein, S., 1992, Global tectonics and space geodesy: Science, v. 256, p. 333-342.

Gregory Wodzicki, K. M., 2000, Uplift history of the central and northern Andes: A review: Geological Society of America Bulletin, v. 112, p. 1091-1105.

Hassani, R., Jongmans, D., Chèry, J., 1997, Study of plate deformation and stress in subduction processes using two-dimensional numerical models, Journal of Geophysical Research, v. 102, p. 17,951-17,965.

Hickman, S. H., 1991, Stress in the lithosphere and strength of active faults, Reviews of Geophysics, v. 29, p. 759-775.

Husson, L., Ricard, Y., 2004, Stress balance above subduction: application to the Andes: Earth and Planetary Science Letters, v. 222, p. 1037-1050.

Kong, X., Bird, P., 1995, SHELLS: A thin-shell program for modeling neotectonics of regional or global lithosphere with faults: Journal of Geophysical Research, v. 100, p. 22,129-22,132.

Lamb, S., Davies, P., 2003, Cenozoic climate change as a possible cause for the rise of the Andes: Nature, v. 425, p. 792-797.

Lithgow-Bertelloni, C., Richards, M. A., 1998, The Dynamics of Cenozoic and Mesozoic Plate Motions: Review of Geophysics, v. 36, p. 27-78.

Molnar, P., England, P., Martinod, J., 1993, Mantle dynamics, uplift of the Tibetan plateau, and the Indian monsoon: Review of Geophysics, v. 31, p. 357-396.

Morgan, W. J., 1968, Rises, trenches, great faults, and crustal blocks: Journal of Geophysical Research, v. 73, p. 1959-1982.

National Geophysical Data Center, Boulder, Colorado, 1998, Data Announcement 88-MGG-02: Digital relief of the surface of the Earth. NOAA.

Norabuena, E. O., Leffler-Griffin, L., Mao, A., Dixon, T. H., Stein, S., Sacks, I. S., Ocola, L., Ellis, M., 1998, Space geodetic observations of Nazca-South America convergence across the central Andes: Science, v. 279, p. 358-362.

Norabuena, E. O., Dixon, T. H., Stein, S., Harrison, C. G. A., 1999, Decelerating Nazca-South America and Nazca-Pacific plate motions: Geophysical Research Letters, v. 26, p. 3405-3408.

Raymo, M. E., Ruddiman, W. F., 1992, Tectonic forcing of late Cenozoic climate: Nature, v. 359, p. 117-122.

Richards, M. A., Engebretson, D. C., 1992, Large-scale mantle convection and the history of subduction: Nature, v. 355, p. 437-440.

Rousse, S., Gilder, S., Farber, D., McNulty, B., Torres, V. R., 2002, Paleomagnetic evidence for rapid vertical-axis rotation in the Perivian Cordillera ca. 8 Ma: Geology, v. 30, p. 75-78.

Sella, G. F., Dixon, T. H., Mao, A., 2002, REVEL: a model for recent plate velocities from space geodesy: Journal of Geophysical Research, v. 107, p. 11,1-11,30.

Sobel, E. R., Hilley, G. E., Strecker, M. R., 2003, Formation of internally drained contractional basins by aridity-limited bedrock incision: Journal of Geophysical Research, v. 108, p. 6,1- 6,23.

Sobolev, S. V., Babeyko, A. Y., 2005, What drives orogeny in the Andes?: Geology, v. 33, p. 617-620.

Somoza, R., 1998, Updated Nazca (Farallon)-South America relative motions during the last 40 My: implications for mountain building in the central Andean region: Journal of South American Earth Sciences., v. 11, p. 211-215.

Song, T.-R. A., Simons, M., 2003, Large trench-parallel gravity Variations predict seismogenic behavior in subduction zones: Science, v.301, p. 630-633.

Tackley, P. J., Stevenson, D. J., Glatzmaier, G. A., Schubert, G., 1994, Effects of multiple phase transitions in a three-dimensional spherical model of convection in Earth's mantle: Journal of Geophysical Research, v. 99, p. 15,877-15,902.

Zhong, S., Zuber, M. T., Moresi, L., Gurnis, M., 2000, Role of temperature-dependent viscosity and surface plates in spherical shell models of mantle convection: Journal of Geophysical Research, v. 105, p. 11,063-11,082.
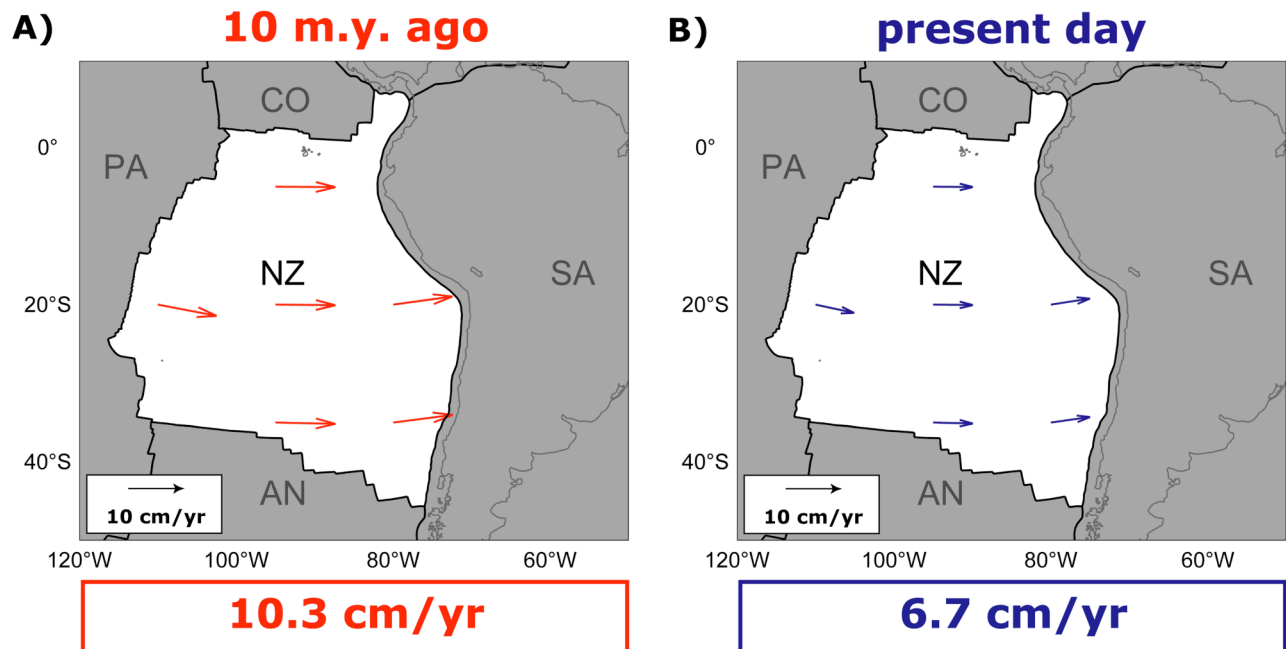
Fig. 1.1. Nazca (NZ) plate motion relative to South America (SA) from Gordon and Jurdy (1986) **(a)** and Norabuena et al. (1999) **(b)**. Plate boundaries are in black, coastlines in gray. Reconstructions show convergence of 10.3 cm/yr at long 71.5° W, lat 25° S; geodetic data indicate 6.7 cm/yr at the same position. Difference implies deceleration of the Nazca plate relative to South America over the last 10 m.y. PA-Pacific; CO-cocos; AN-Antarctica.
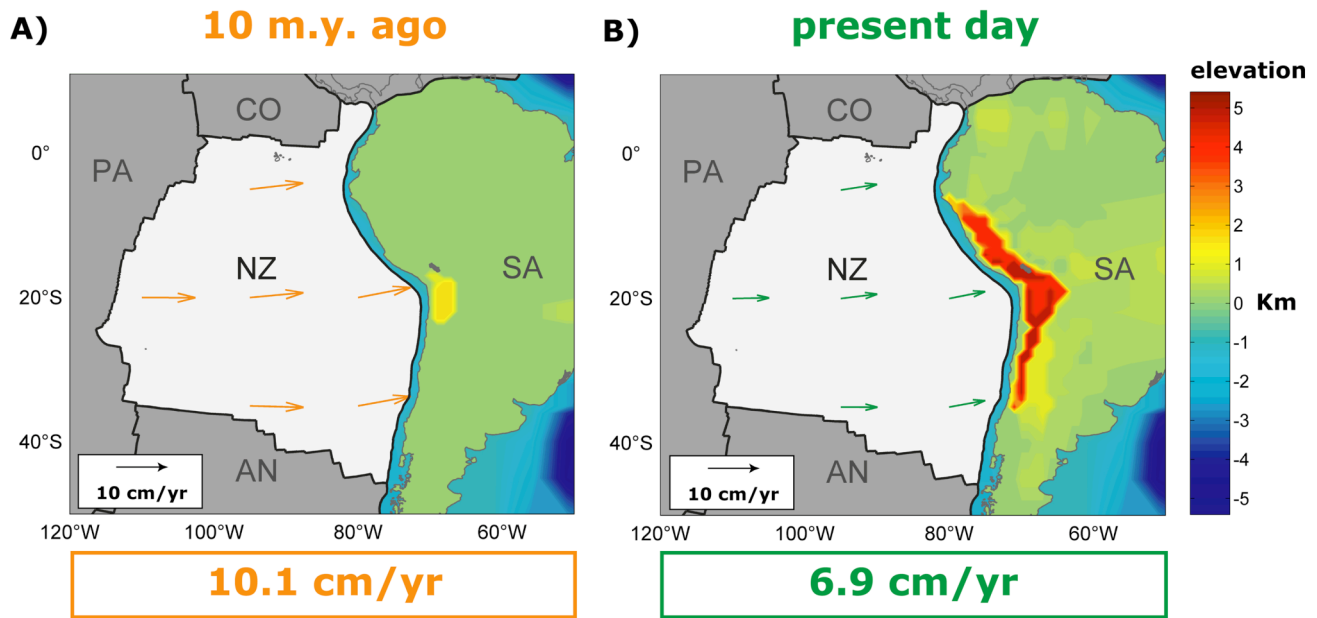
Fig. 1.2. Computed Nazca (NZ) plate motion relative to South America (SA) from global plate motion simulations corresponding to assumed Andean paleotopography 10 m.y. ago **(a)** and present-day topography **(b)** from ETOPO 5 data set (National Geophysical Data Center, 1998). Abbreviations as in Fig. 1.1. Plate boundaries are in black, coastlines and lakes are in gray. Assumed paleotopography 10 m.y. ago results in computed convergence of 10.1 cm/yr at long 71.5°W, lat 25°S; present-day topography results in convergence of 6.9 cm/yr at same position. Difference implies that deceleration of Nazca plate is due to topographic load of Andes (see text).
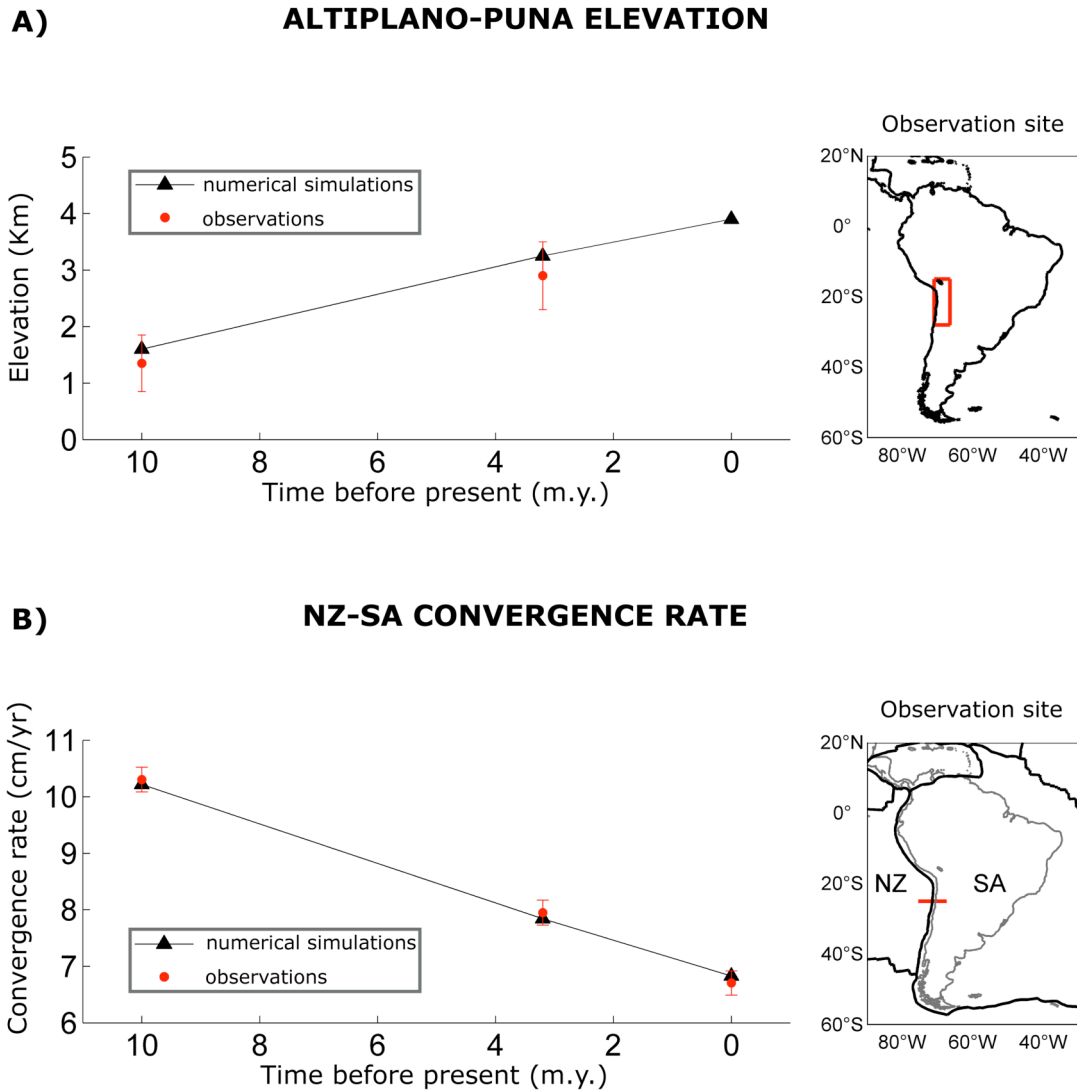
Fig. 1.3. Published estimates of Andean paleotopography **(a)** and Nazca–South America (NZ-SA) plate convergence **(b)** for past 10 m.y. (see text) marked by red dots with error bounds. Black triangles - computed plate convergence and corresponding model topography for Andes. Observations show inverse correlation of plate velocity and elevation of Altiplano-Puna plateau, which is confirmed quantitatively by our simulations.
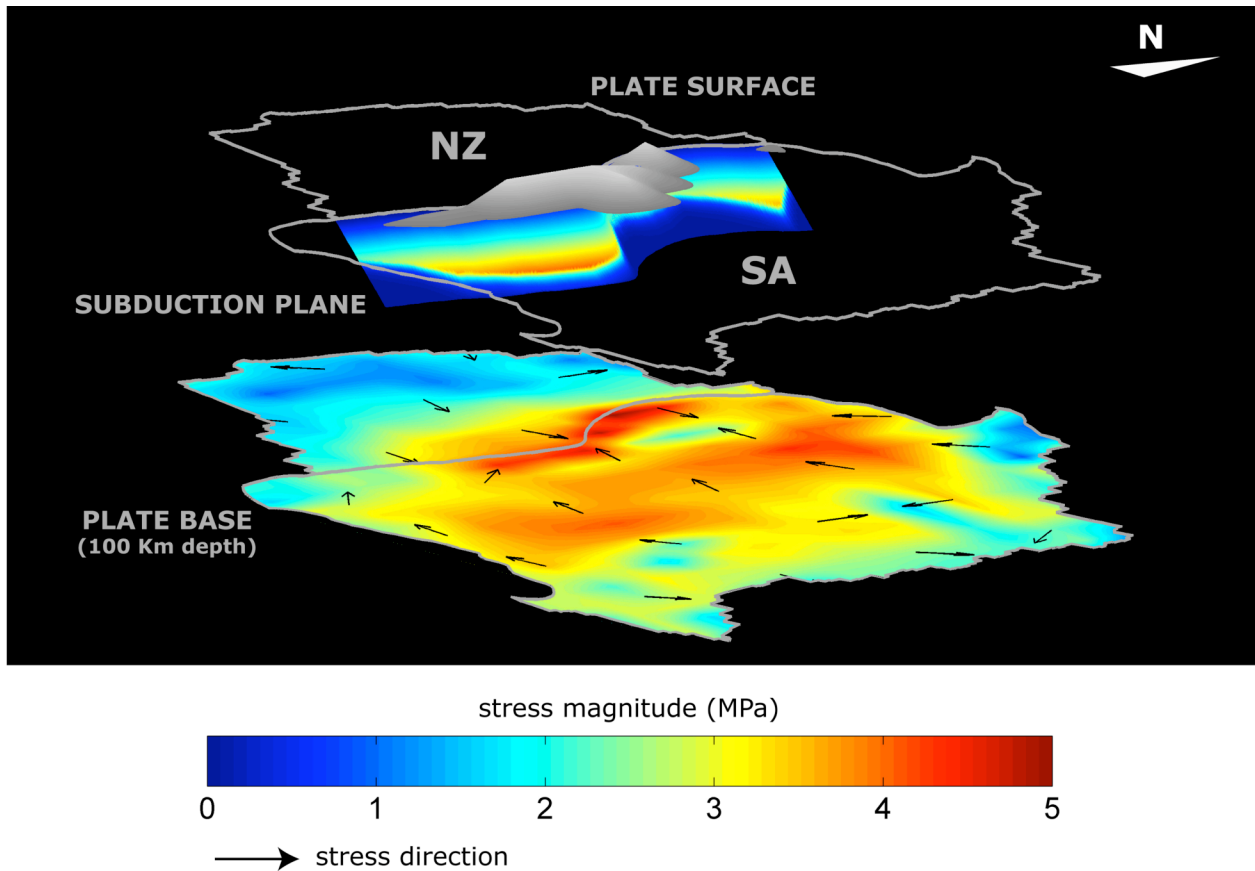
Fig. 1.4. Subduction plane and plate base stresses at present day inferred from our simulation for Nazca (NZ) and South America (SA) plates. Color scale indicates stress magnitude (in MPa), arrows indicate stress direction. Plate boundaries (bottom) and Andes topographic contour lines (top) are in gray. Note that resisting stresses along subduction plane are comparable in magnitude to plate driving shear tractions from mantle, especially under highly elevated regions in the central Andes. Frictional forces at plate boundary are raised by $1*10**13$ N/m due to growth of the Andes.
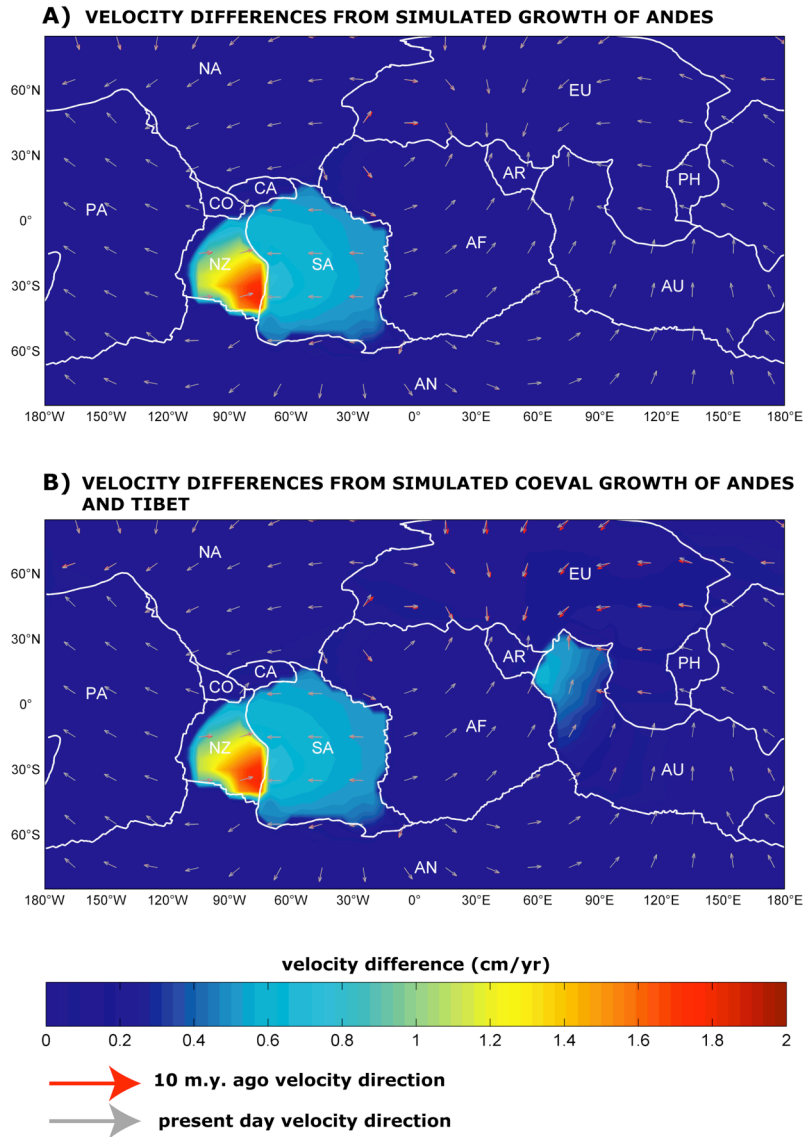
Fig. 1.5. (a): Difference of global plate velocities between model simulation with assumed Andean paleotopography 10 m.y. ago and calculation with present-day topography. Color scale is in cm/yr; arrows indicate velocity direction in hotspot reference frame. Plate boundaries are marked in white. Effect of topography on plate motion is spatially confined to plates sharing convergent margin. PA-Pacific; NA-North America; CO-Cocos; CA-Caribbean; AN-Antarctica; AF-Africa; AR-Arabia;

EU-Eurasia; PH-Phillippine; AU-Australia. **(b)**: Same as A but for simulated coeval growth of Tibet. Growth of Tibet does not significantly alter our estimates for change in Nazca–South America (NZ-SA) convergence.

Chapter 2

Mountain belt growth inferred from histories of past plate convergence: a new tectonic inverse problem

Summary

Past plate motions display a range of variability, including speedups and slowdowns that cannot easily be attributed to changes in mantle related driving forces. One key controlling factor for these variations is the surface topography at convergent margins, as previous modeling shows that the topographic load of large mountain belts consumes a significant amount of the driving forces available for plate tectonics by increasing frictional forces between downgoing and overriding plates. Here we use this insight to pose a new tectonic inverse problem and to infer the growth of mountain belts from a record of past plate convergence. We introduce the automatic differentiation method, which is a technique to produce derivative code free of truncation error by source transformation of the forward model. We apply the method to a publicly

available global tectonic thin-shell model and generate a simple derivative code to relate Nazca/South America plate convergence to gross topography of the Andes mountain belt. We test the code in a search algorithm to infer an optimal paleotopography of the Andes 3.2 m.y. ago from the well-known history of Nazca/South America plate convergence. Our modeling results are in excellent agreement with published estimates of Andean paleotopography and support the notion of strong feedback between mountain belt growth and plate convergence.

INTRODUCTION

Computer models of the lithosphere are a powerful tool in tectonics. They allow us to identify key controlling parameters from forward simulations and to constrain their values through an inverse modeling approach. One potentially important parameter in regulating the velocity of tectonic plates is the topography of large mountain belts along their margins. At the Nazca/South America (NZ/SA) plate boundary, for example, recent tectonic simulations show a 30% reduction in plate convergence following the Miocence/Pliocene uplift of the Puna and Altiplano plateaus [Iaffaldano et al., 2006]. The simulations link the velocity reduction explicitly to frictional forces along the brittle portion of the plate boundary arising from the overburden pressure of

the newly raised topography. They are in excellent agreement with paleomagnetic and geodetic measures of NZ/SA plate convergence. The recent reduction in NZ/SA convergent rate is not an isolated episode of a rapid change in plate motion. In fact, such changes are well documented from detailed paleomagnetic reconstructions of oceanic spreading rates. Fig. 2.1 shows a recent compilation of global sea floor spreading half-rates [Whittaker and Müller, 2006]. It is evident that the record is characterized by a number of abrupt variations in plate velocities throughout the past 180 m.y. Moreover, the global positioning system (GPS) now allows us to derive precise estimates of present-day motions [Dixon, 1991]. Such measurements reveal a number of plate motion changes even on relatively short time-scales, on the order of a few m.y. This is evident from Fig. 2.2, where we compare global plate motions over the past 3.2 m.y. from the paleomagnetic reconstruction NUVEL-1A [DeMets et al., 1994] relative to the geodetic compilation REVEL [Sella et al., 2002]. Fig. 2.2 reveals significant plate motion change, for example for the India, Nazca, and South America plates, over the past 3.2. m.y. Those variations cannot easily be attributed to changes in mantle related driving forces, because the global mantle circulation system operates much too sluggish to vary significantly on time scales of a few million years and probably undergoes changes on a much longer time scale on the order of 100-200 m.y. [Bunge et al. 1998]. A likely key controlling factor for short-term plate motion variations, however, are rapid variations in surface topography at convergent margins.

This is because the topographic load of large mountain belts consumes a significant amount of the driving forces available for plate tectonics as noted above. The observation suggests to explore a novel inverse problem and to infer mountain belt paleotopography from a record of past plate convergence. Here we follow this approach and apply estimates of the NZ/SA plate convergence history to infer past topography of the Andes. The theoretical predictions are verified explicitly against a range of Andean paleotopography estimators. Inverse problems are, of course, well known in the Earth sciences where one often must infer one set of model parameters from a related set of measurements [Tarantola, 1987; 2004]. In seismology they date back more than 30 years, when Backus and Gilbert [1968] studied the resolving power of gross earth data. In tectonic studies inverse methods are used frequently to constrain the kinematics of plate motion through the growing body of data from the global positioning system (GPS) [Bennett et al., 2004], although their use in dynamic models of the lithosphere is still in its infancy. Inverse techniques rely on an objective function, J, which maps differences between model predictions and observables to a scalar through a sum of integrals. The necessary condition for an optimum of J, that grad J = 0, requires the differentiation of the forward model with respect to the unknown parameters. A straightforward way to obtain grad J is through finite differencing of the forward model. Unfortunately, the method of computing model sensitivities by divided differences is prone to truncation error and involves the

difficulty of determining a suitable step size to balance truncation and cancellation errors. Moreover, it consumes large amounts of computer time especially in numerical simulations involving millions of degrees of freedom. Here the use of an adjoint technique is computationally attractive [Bunge et al., 2003]. But the approach requires the analytic derivation of an adjoint and manually written code. In contrast, the technique of Automatic Differentiation is a method for automatically generating programs to compute derivatives [Rall, 1981]. In the Automatic Differentiation approach a computer program evaluating a function representing the forward problem is mechanically transformed into another computer program capable of evaluating the Jacobian or higher order derivatives of the function [Griewank, 2000]. Automatic Differentiation exploits the fact that every computer program, no matter how complicated, executes a sequence of elementary arithmetic operations and that by applying the chain rule of derivative calculus repeatedly to these operations, derivatives of arbitrary order can be computed automatically and accurate to working precision. In addition, the automatic nature of the approach allows for straightforward integration of new physical processes and constraints into a model without need for further human intervention. This makes the method well suited for a wide range of computer simulations across the earth sciences [Bischof et al., 1996a; Sambridge et al., 2005; Rath et al., 2006]. In this paper we apply the Automatic Differentiation tool ADIFOR [Bischof et al., 1996b] (see www.autodiff.org) in the so-called forward mode

to a publicly available global plate tectonic model (SHELLS) [Kong and Bird, 1995]. Our goal is to accurately infer an optimal paleotopography in the Andes some 3 m.y. ago that is consistent with the record of recent NZ/SA America plate convergence. An indication of the gross value of the Andean topography at the same age has in fact been inferred in a previous study [Iaffaldano et al., 2006] by applying a simple derivative-free line search. The approach presented here is emphatically not intended to explore the full capabilities of the Automatic Differentiation approach, because there are still large uncertainties associated with estimating paleotopography. Rather we wish to explore whether the sensitivity information obtained from our approach can be used successfully to constrain tectonic modeling parameters. To this end we focus our attention deliberately on a tectonic problem for which the first-order model sensitivity has been mapped from previous forward simulations, testing the hypothesis that temporal variations in plate convergence could potentially serve as a proxy for the evolution of gross topography in mountain belts.

MODEL AND RESULTS

Fig. 2.3 shows observed Nazca plate motion relative to South America 10 m.y. ago (a) and today (b). Paleomagnetic reconstructions indicate a convergence of (10.3 ± 0.2

cm/yr) at (71.5° W, 25° S) [Gordon and Jurdy, 1986], whereas the current value obtained from geodetic data is (6.7 ± 0.2 cm/yr) at the same location [Norabuena et al., 1998], consistent with an overall velocity reduction of about 30% over the past 10 m.y. Fig. 2.3 also shows the result of two global plate tectonic computer simulations. The simulations are performed using the SHELLS code. It employs isostasy through the Airy compensation [Bird, 1998]. A complete representation of lithosphere strength requires a 3-D volume approach; however for large-scale tectonic problems it is reasonable to assume that the horizontal velocity component to first order is independent of depth and to use a vertical integration of lithospheric strength down to a depth consistent with the Airy compensation. Such approach reduces the 3-D problem to two dimensions [Bird, 1989], in what is known as thin-shell approximation. We account for realistic plate driving forces from global mantle circulation modeling [Bunge et al., 1998, 2002] and include topography, a temperature-dependent viscous rheology and faults along plate margins to accommodate Coulomb frictional sliding in the cold brittle portion of the lithosphere and dislocation creep in the warm ductile regions. The computed Nazca/South America convergence is 10.1 cm/yr for paleotopography corresponding to conditions 10 m.y. ago (c), whereas the current elevation of the Andes [National Geophysical Data Center] results in a computed plate convergence of 6.9 cm/yr (d). Note that the assumed change in topography of the Andes is the only difference between (c) and (d)

41

and that it is associated with an increase of frictional resting forces along the plate margin to tectonically significant values as high as 2*10**13 N/m [Iaffaldano et al., 2006]. The modeled plate velocities agree with the recorded plate motions in (a) and (b) at the 68% confidence level. Next to the observations from Gordon and Jurdy and Norabuena et al., there is a velocity constraint available at 3.2 m.y. on Nazca/South America plate convergence from the global plate motion reconstruction NUVEL-1A. The record is based on paleomagnetic data and indicates a convergence of (8 ± 0.2 cm/yr), faster than the current rate but slower than the convergence 10 m.y. ago. We use this constraint to perform a numerical inversion of the tectonic model. In our approach we take the ADIFOR tool to generate a derivative code of SHELLS and apply the code in an iterative bisection search to infer an optimal paleoelevation of the Andes 3.2 m.y. ago. The optimum refers to an elevation resulting in a model-predicted plate convergence that agrees with the recorded convergence rate of NUVEL-1A. Specifically we compute the derivative in the tectonic model of the Squared misfit between observed and modeled Nazca/South America plate convergence relative to Andean topography at 3.2 m.y.:

$$Squared\ misfit(e) = (Conv\_obs - Conv\_sml(e))**2$$

Here Conv_obs is the observed convergence from NUVEL-1A and Conv_sml(e) is the modeled convergence from SHELLS (when used to perform forward simulations) for an assumed Andean paleoelevation denoted by e. The above expression is nothing but the squared distance between the observed and modeled plate convergence and provides us with a convenient misfit function of how any given Andean paleoelevation relates to a modeled plate convergence at 3.2 m.y. We sketch the qualitative behavior of the Squared misfit in the inset of Fig. 2.4. Note that the Squared misfit is positive by construction and that unrealistic paleoelevations of the Andes (either too high or too low) result in large values of the Squared misfit, with an optimum leading to a zero value. Fig. 2.4 shows the derivative of the Squared misfit relative to a range of assumed paleoelevations of the Andes at 3.2 m.y. It is worth to notice that we express the elevation of the Andes with one single scalar parameter which is the percentage of the local topographic growth since 10 m.y., with 0% topographic growth being the topography at 10 m.y. (Fig. 2.3c) and 100% topographic growth corresponding to the elevation of the Andes today (Fig. 2.3d) at any location. Thus, the same percentage of topographic growth will correspond to different elevations in different locations of the Andean region, depending on the present-day as well as 10 m.y. ago elevation of those locations. This is a convenient way to relate the Squared misfit to one single parameter representative of the whole assumed Andean topography. We note from Fig. 2.4 that the derivative of the Squared misfit crosses from negative to positive values in the

range of 70-80% overall topographic growth and that the zero value (an optimum in the misfit function, see inset Fig. 2.4) occurs at about 75% of the total topographic growth. The iterative bisection search locates the optimum within 5 iterations. Thus we infer the optimal elevation of the Andes with respect to Nazca/South America plate convergence at 3.2 m.y. at about 75% of total topographic growth over the past 10 m.y. We plot this theoretical prediction of Andean paleotopography in Fig. 2.5.

DISCUSSION

It is logical to ask whether our prediction is supported by independent estimators of paleotopography in the Andes. We address this question in Fig. 2.6. Here we compare our inverse modeling result with published estimates of Andean paleotopography based on paleobotanical data for the Altiplano (Fig. 2.6a) and Eastern Cordillera (Fig. 2.6b) regions [Gregory Wodzicki, 2000]. We find that the predicted paleoelevation from our numerical inversion for both the Altiplano and the Eastern Cordillera at 3.2 m.y. agrees well with paleotopographic indicators to within the (admittedly wide) error range (see Fig. 2.6). Such results also agree with findings from forward models of NZ/SA convergent rate addresses in our previous study, where we inferred the gross Andean topography 3.2 m.y. ago by performing a derivative-free line search.

Moreover, our inverse simulation supports a separate timing in the uplift history of the Eastern Cordillera relative to the Altiplano, with rapid uplift commencing somewhat later in the Eastern Cordillera than in the Altiplano. A staggered uplift activity of the Eastern Cordillera relative to the Altiplano has been suggested before [Gregory Wodzicki, 2000; Ghosh et al., 2006]. The Altiplano plateau, for example, had achieved less than half its present elevation 10 m.y. ago and subsequently saw an uplift of about 0.25 mm/yr during the late Miocene, reaching an elevation of about 3 Km by 3.2 m.y. (Fig. 2.6a). The Eastern Cordillera in contrast had achieved an elevation of less than 1 Km 10 m.y. ago and was uplifted primarily during the Pliocene at rates of about 0.9 mm/yr (Fig. 2.6b). In our discussion we must remark upon numerical accuracy and computational cost of the Automatic Differentiation approach. The crucial advantage of this numerical technique over divided difference lies in its accuracy, which is essential to assure efficient convergence in an iterative optimization [Sinha et al., 1999]. We verified that the truncation error in the value of the derivative incurred by divided differences exceeds 10% for a step size of 10**-2, especially near the optimum of the misfit function. The error reduces to less than a percent for smaller step sizes in the range of 10**-3 to 10**-7, but increases again upon further reduction thus confirming the difficulty of finding an optimal step size for divided difference even for the relatively simple problem we consider here. In contrast, there is no truncation error in the Automatic Differentiation approach. In our study we used AD to

compute the derivative of the misfit between observed and modeled plate convergence with respect to a single model parameter, the paleoelevation of the Andes 3.2 m.y. ago. For the derivative code we measure an execution time of 370s, whereas the forward simulation executes in 195s. The ratio of the execution times is 1.9, roughly comparable to numerical differentiation based on divided differences which would require two runs of the forward model. We obtain this performance without further modifying the derivative code, even though performance optimization would certainly help to improve its execution time. Thus straightforward application of the ADIFOR tool leads to a performance comparable to the fastest divided difference.

CONCLUSION

We have produced a derivative code capable of computing gradients free of truncation error by applying the AD tool ADIFOR to the publicly available thin-shell model SHELLS. The approach combines the generality of finite difference techniques and the accuracy of analytical derivatives, while at the same time eliminating `human' coding errors. We think that the technique of Automatic Differentiation has considerable potential for nonlinear optimization, linearizing of nonlinear inverse problems as well as for sensitivity analysis in tectonic computer simulations. Our model prediction of

Andean paleotopography at 3.2 m.y. from records of Nazca/South America plate convergence agrees with independent paleotopographic estimators and supports the notion of strong feed back between mountain belt growth and plate convergence.

REFERENCES

Backus, G. E., Gilbert, J. F., 1968, The resolving power of gross earth data: Geophysical Journal of the Royal Astronomical Society, v. 16, p. 169-205.

Bennett, R. A., Friedrich, A. M., Furlong, K. P., 2004, Codependent histories of the San Andreas and San Jacinto fault zones from inversion of fault displacement rates: Geology, v. 32, p.961-964.

Bird, P., 1989, New finite element techniques for modeling deformation histories of continents with stratified temperature-dependent rheology: Journal of Geophysical Research, v. 94, p. 3967-3990.

Bird, P., 1998, Testing hypotheses on plate-driving mechanisms with global lithosphere models including topography, thermal structure, and faults: Journal of Geophysical Research, v. 103, p. 10,115-10,129.

Bischof, C., Pusch, G., Knoesel, R., 1996a, Sensitivity analysis of the MM5 weather model using automatic differentiation: Computers in Physics, v. 10, p. 605-612

Bischof, C., Carle, A., Khademi, P., Mauer, A., 1996b, Adifor 2.0: Automatic differentiation of Fortran 77 programs: IEEE Computational Science & Engineering, v. 3, p. 18-32.

Bunge, H.-P., Richards, M.A., Lithgow-Bertelloni, C, Baumgardner, J.R., Grand, S., Romanowicz, B., 1998, Time scales and heterogeneous structure in geodynamics earth models: Science, v. 280, p. 91-95.

Bunge, H-P., Richards, M. A., Baumgardner, J. R., 2002, Mantle circulation models with sequential data-assimilation: inferring present-day mantle structure from plate motion histories: Phil. Trans. Roy. Soc. A, v. 360, p. 2545-2567.

Bunge, H-P., Hagelberg, C. R., Travis, B. J., 2003, Mantle circulation models with variational data-assimilation: inferring past mantle flow and structure from plate motion histories and seismic tomography: Geophysical Journal International, v. 152, p. 280-301.

DeMets, C., Gordon, R. G., Argus, D. F., Stein, S., 1994, Effect of recent revisions to the geomagnetic reversal time scale on estimates of current plate motions: Geophysical Research Letters, v. 21, 2191-2194.

Dixon, T. H., 1991, An introduction to the Global Positioning System and some geological applications: Reviews of Geophysics, v. 29, p. 249-276.

Ghosh, P., Garzione, C. N., Eiler, J. M., 2006, Rapid Uplift of the Altiplano Revealed Through 13C-18O Bonds in Paleosol Carbonates: Science, v. 311, p. 511-515.

Gordon, R. G., Jurdy, D. M., 1986, Cenozoic global plate motions: Journal of Geophysical Research, v. 91, p. 12,389-12,406.

Gregory Wodzicki, K. M., 2000, Uplift history of the central and northern Andes: A review: Geological Society of America Bulletin, v. 112, p. 1091-1105.

Griewank, A., 2000, Evaluating Derivatives: Principles and Techniques of Algorithmic Differentiation: SIAM, Philadelphia.

Iaffaldano, G., Bunge, H-P., Dixon, T. H., 2006, Feedback between mountain belt growth and plate convergence: Geology, v. 34, p.893-896.

Kong, X., Bird, P., 1995, SHELLS: A thin-shell program for modeling neotectonics of regional or global lithosphere with faults: Journal of Geophysical Research, v. 100, p. 22,129-22,132.

National Geophysical Data Center, Boulder, Colorado, 1998. Data Announcement 88-MGG-02: Digital relief of the surface of the Earth. NOAA.

Norabuena, E. O., Leffler-Griffin, L., Mao, A., Dixon, T. H., Stein, S., Sacks, I. S., Ocola, L., Ellis, M., 1998, Space geodetic observations of Nazca-South America convergence across the central Andes: Science, v. 279, p. 358-362.

Rall, L. B., 1981, Automatic differentiation: Techniques and applications: Lecture notes in computer science, v. 120, Berlin, Springer Verlag.

Rath, V., Wolf, A., Bücker, H. M., 2006, Joint three-dimensional inversion of coupled groundwater flow and heat transfer based on automatic differentiation: Sensitivity calculation, verification and synthetic examples: Geophysical Journal International, in press.

Sambridge, M.; Rickwood, P.; Rawlinson, N., 2005, Automatic Differentiation in Geophysical Inverse Problems: American Geophysical Union, Fall Meeting 2005, abstract #NG42A-02

Sella, G. F., Dixon, T.H., Mao, A., 2002, REVEL: A model of Recent plate velocities from space geodesy: Journal of Geophysical Research, v. 107, p. ETG 11,1-11,12.

Sinha, A., Rao, B.V., Bischof, C., 1999, Nonlinear optimization model for screening multipurpose reservoir systems: Journal of Water Resources Planning and Management, v. 125, p. 229-233

Tarantola, A., 1987, A strategy for nonlinear elastic inversion of seismic-reflection data: Geophysics, v. 52, p. 429-429.

Tarantola, A., 2004, Inverse problem theory. Methods for model parameter estimation: SIAM, Philadelphia.

Whittaker, J., Müller, D., 2006, New 1-minute satellite altimetry reveals major Australian-Antarctic plate reorganization at Hawaiian-Emperor bend time: American Geophysical Union Fall Meeting.

History of ocean floor spreading for the past 180 m.y.

Spreading half-rate (mm/yr)
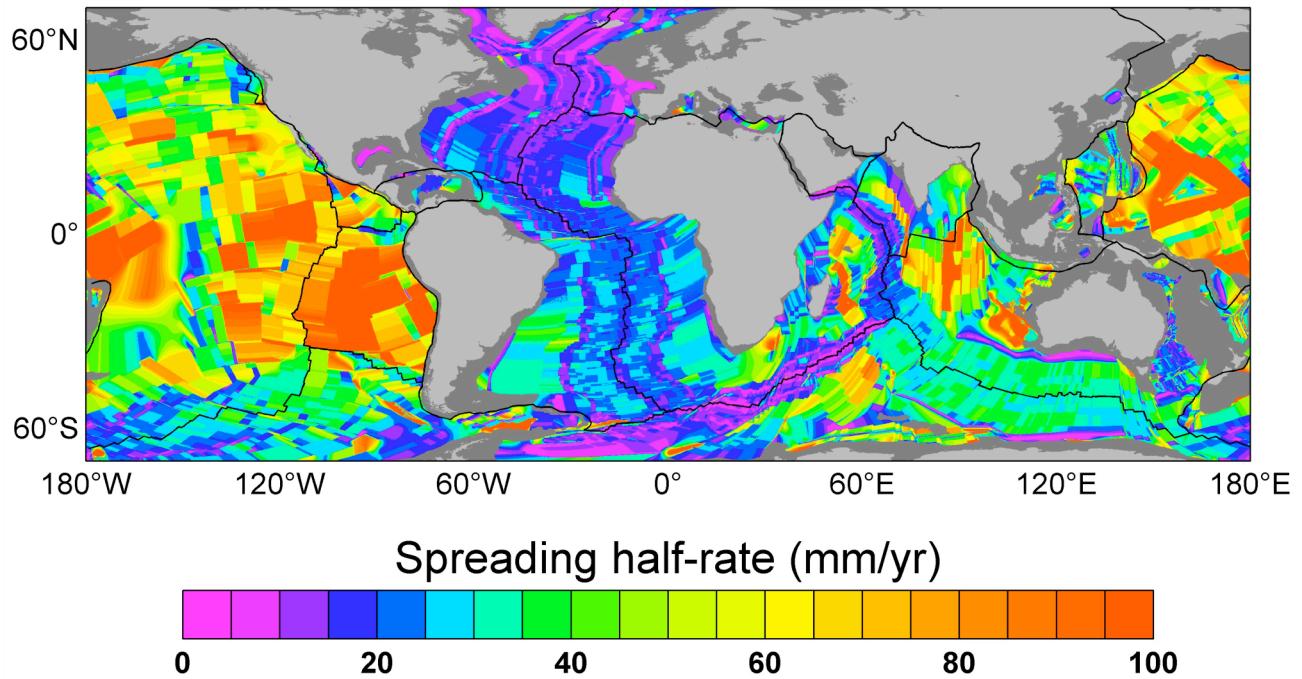
Fig. 2.1. Spreading half-rates for the past 180 m.y. after a recent global compilation by Whittaker and Müller. Abrupt changes in global spreading rates reveal short-term variations in plate motions. These are probably not due to changes in mantle driving forces, which occur on a much longer time scale of the order of 50 to 100 m.y. as indicated by global mantle circulation models (see text), and are likely related to short-term variations in plate boundary forces caused, for example, by rapid variations in surface topography at convergent margins. Global plate boundaries are in black, continental lithosphere in light gray.
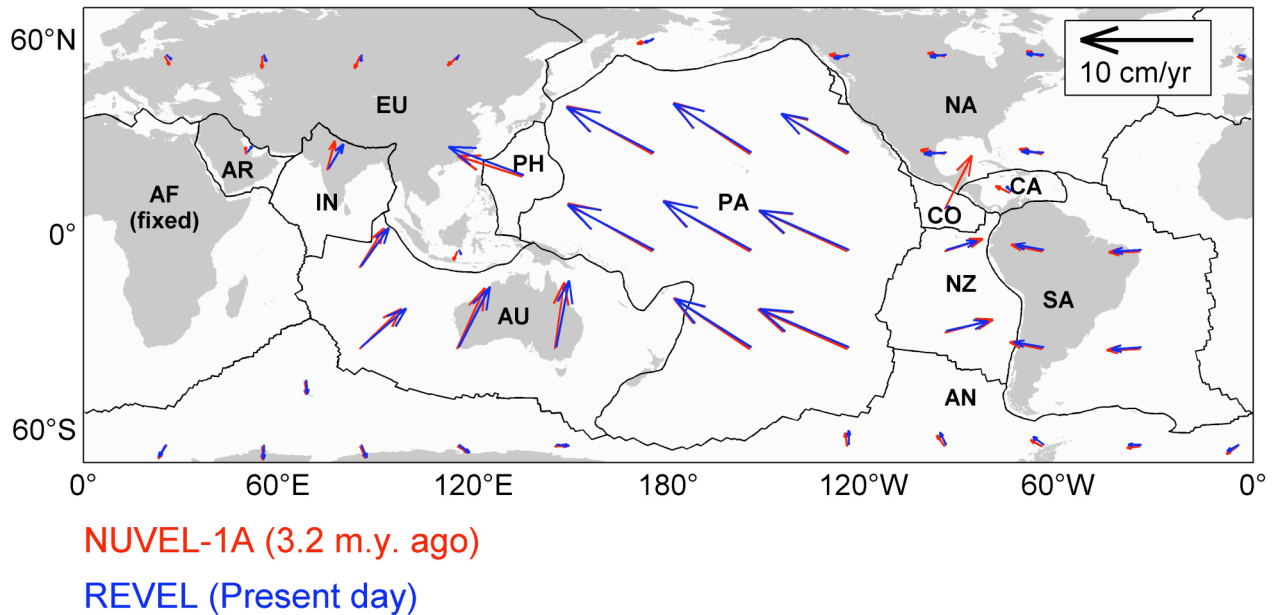
Fig 2.2. Comparison of plate motion models over the past 3.2 m.y. derived from paleomagnetic (NUVEL-1A, in red) observations with instantaneous geodetic (REVEL, in blue) estimates. Global plate motions reveal significant short-term variations even for the most recent plate motion history, which are unlikely related to changes in mantle driving forces and most probably due to plate boundary forces. There are significant directional changes for the India (IN) plate, as well as changes in the magnitude of motion for Nazca (NZ) and South America (SA) plates. Velocity vectors are plotted in a reference frame fixed with rigid Africa (AF) plate. Plate boundaries are in black, continents are in gray. Plate abbreviations: AN-Antarctica, AR-Arabia, AU-Australia, CA-Carribean, CO-Cocos, EU-Eurasia, NA-North America, PA-Pacific, PH-Philippine.

OBSERVED PLATE VELOCITY

a) **10 m.y. ago**
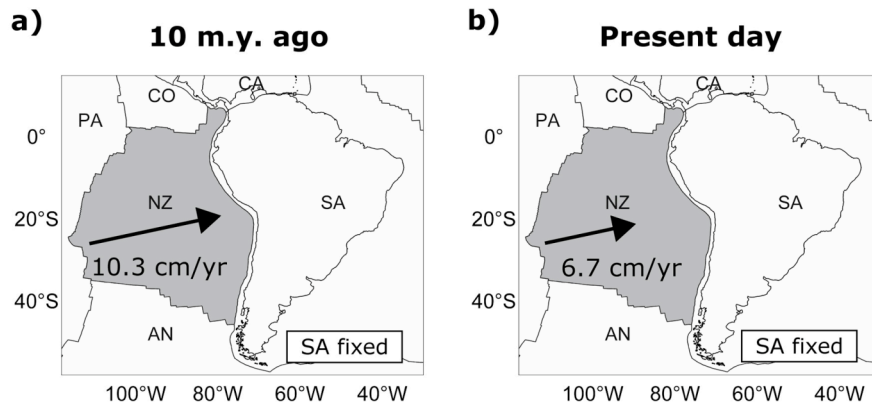
b) **Present day**

PREDICTED PLATE VELOCITY

c) **10 m.y. ago**
(elevation from paleo-estimations)

d) **Present day**
(elevation from ETOPO5 dataset)

Andes elevation (Km)
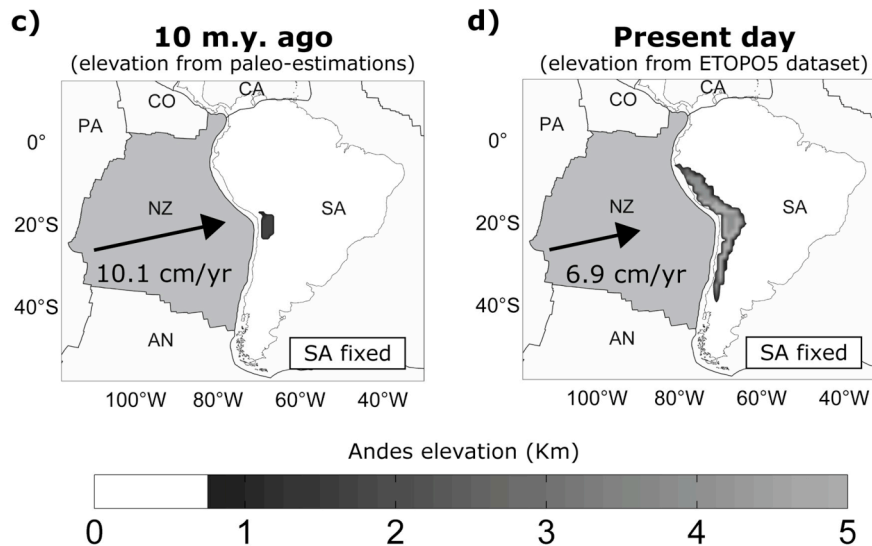
Fig. 2.3. Observed convergence rate between Nazca (NZ) and South America (SA) plates at (71.5° W, 25° S) 10 m.y. ago **(a)** and at present day **(b)**. Observations reveal a velocity reduction of about 30% over the past 10 m.y. Computed Nazca plate motion relative to South America from global plate motion simulations corresponding to Andean paleotopography 10 m.y. ago **(c)** and present-day topography **(d)**. Paleotopography 10 m.y. ago results in a computed convergence rate of 10.1 cm/yr at

the same position, while present-day topography results in a convergence rate of 6.9 cm/yr. The difference implies that the deceleration of the Nazca plate is due to the topographic load of the Andes (see text). Colorscale enhances areas above 700 m altitude. Plate boundaries are in gray, coastline is in black. Plate abbreviations as in Fig. 2.2.
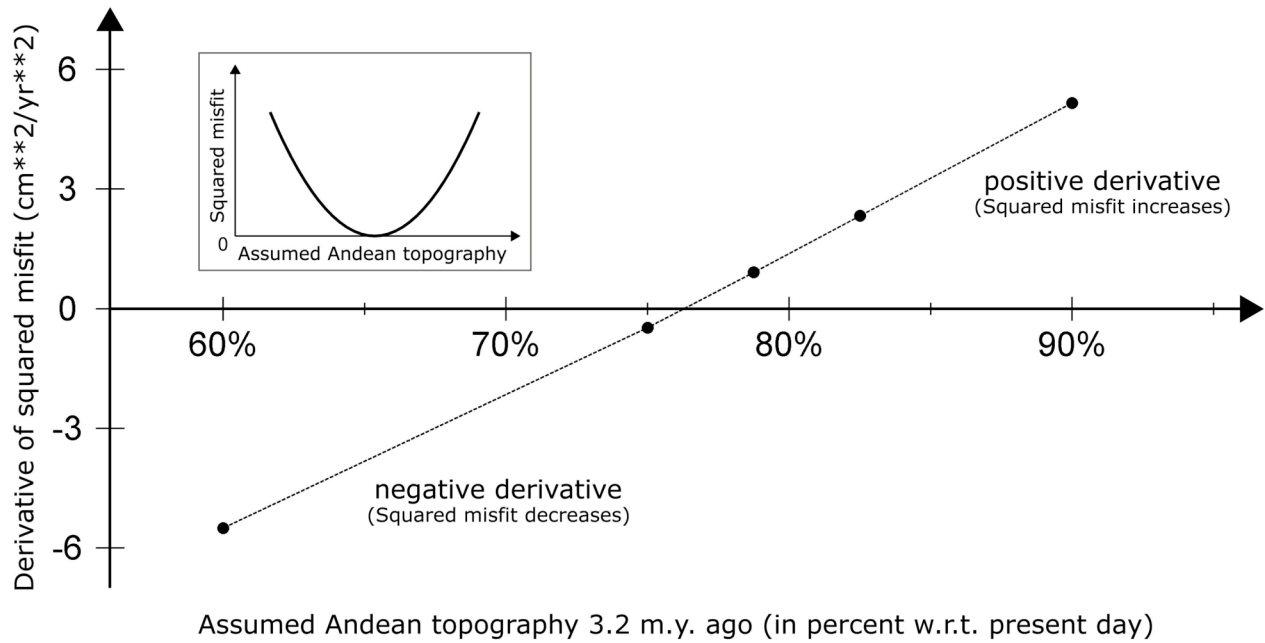
Fig. 2.4. AD-computed derivatives of convergence Squared misfit with respect to assumed Andean topography 3.2 m.y. ago (in percent with respect to present-day elevation). Squared misfit is defined as the squared difference between observed and modeled Nazca/South America convergence rate 3.2 m.y. ago (see text). An illustrative sketch of the Squared misfit trend with respect to assumed Andean topography 3.2 m.y. ago is shown in the inset figure. The iterative bisection search locates the zero of derivative (i.e. minimum of squared misfit) within 5 iterations in the range of 70% - 80%. Thus the optimal topography corresponds to about 75% of the total topographic growth over the past 10 m.y.

Predicted Andes topography 3.2 m.y. ago
(~75% of today)
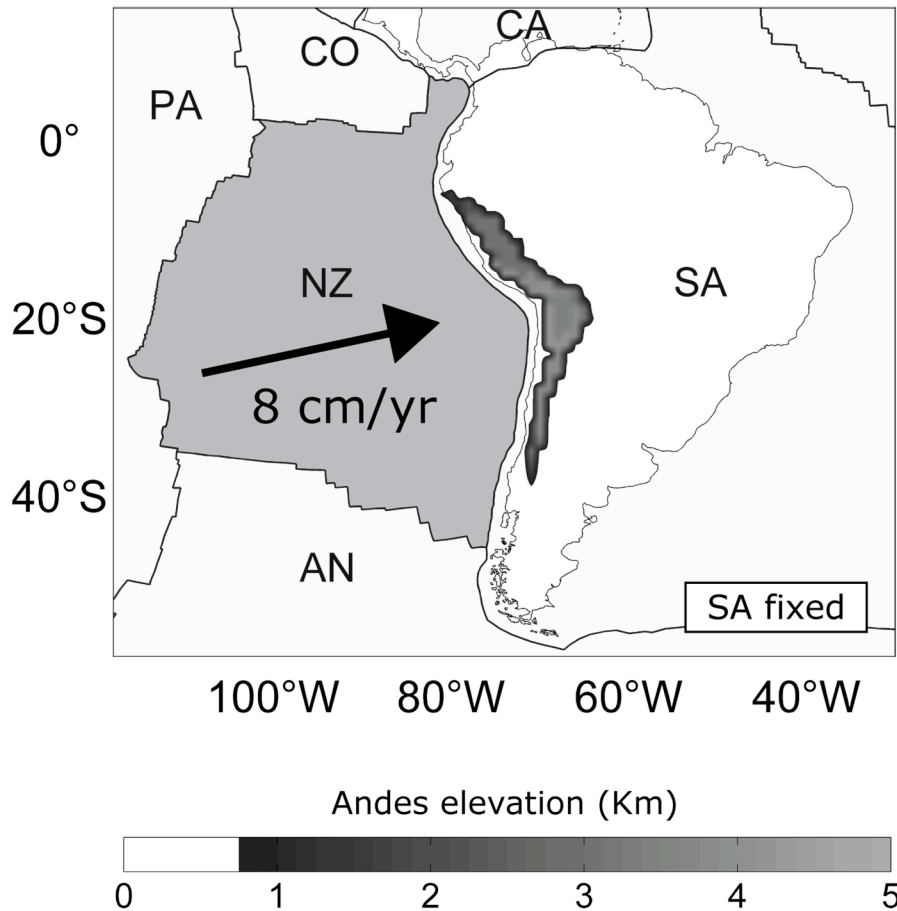
Fig. 2.5. Optimal Andean topography 3.2 m.y. ago inferred through AD. Optimal paleotopography results in 8 cm/yr convergence rate between the Nazca and South America plates, where the convergence velocity is consistent with the NUVEL-1A plate motion reconstruction at the 95% confidence level.

UPLIFT HISTORY

A) ALTIPLANO

B) EASTERN CORDILLERA
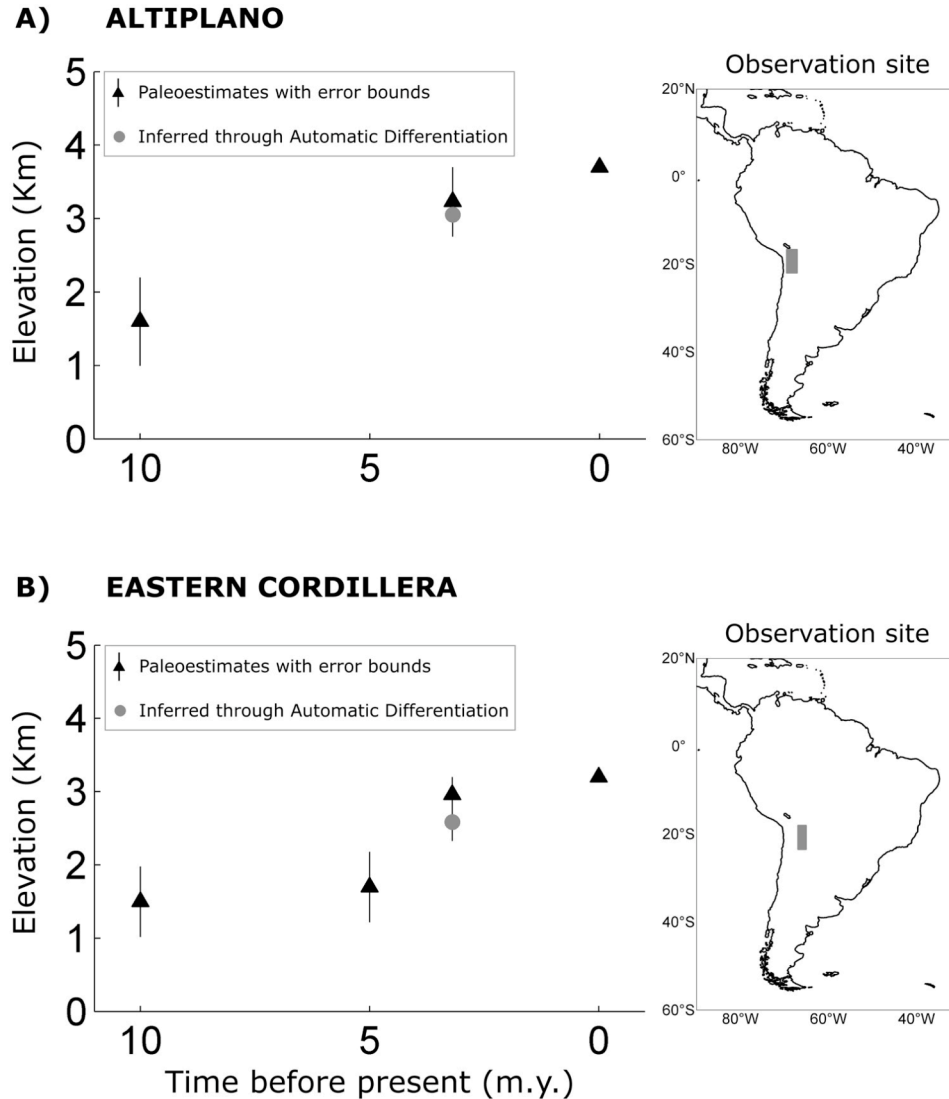
Fig. 2.6. Published estimates of Altiplano **(a)** and Eastern Cordillera **(b)** topography over the last 10 m.y. marked by black triangles with error bounds. AD-inferred optimal topography at 3.2 m.y. is indicated by gray dots. Optimal Andean paleotopography agrees well with independent paleotopographic estimators within the error range and supports a separate timing in the uplift of the Eastern Cordillera relative to the

Altiplano, with rapid uplift commencing somewhat later in the Eastern Cordillera than

in the Altiplano (see text).

Chapter 3

Strong plate coupling along the Nazca/South America convergent margin

SUMMARY

The force balance in plate tectonics is fundamentally important, but poorly known. Here we show that two prominent and seemingly unrelated observations - trench parallel gravity anomalies along the Nazca/South America margin that coincide with the rupture zones of great earthquakes, and a rapid slow down of Nazca/South America convergence over the past 10 m.y. - provide key insights. Both result from rapid Miocene/Pliocene uplift of the Andes and provide quantitative measures on magnitude and distribution of plate coupling along the Nazca/South America margin. We compute the plate tectonic force budget in global models of the faulted lithosphere coupled to high-resolution mantle circulation models and find that Andean-related plate margin forces are comparable to plate driving forces from the mantle and of sufficient magnitude to

account for pronounced bathymetry variations along the trench. Our results suggest that plate coupling, gravity anomalies and bathymetry variations along a given trench are all controlled by long-term stress variations in the upper portion of plate boundaries and that an explicit budget of driving and resisting forces in plate tectonics can be obtained. For the convergent margin considered here, spatial variations in the effective coefficient of friction associated with the distribution of lubricating sediments entering the trench are, by comparison, of minor importance.

INTRODUCTION

Plate tectonics [Morgan, 1968] is remarkable in that it explains the surface motion of the Earth with great accuracy [DeMets et al., 1994], even though the budget of plate driving and resisting forces is poorly known [Forsyth and Uyeda, 1975]. Mantle convection is commonly accepted as the engine for plate motion [Ricard and Vigny, 1989], but the magnitude and distribution of resisting plate margin forces is less clear. Short-term plate motion changes on the order of a few million years or less, which are increasingly revealed through the comparison of geodesy-based measurements [Dixon, 1991; Stein, 1993] and increasingly detailed paleomagnetic reconstructions [Mueller et

al., 2008], represent a powerful probe to quantify these forces. Since rapid plate velocity variations are unlikely to result from changes in the pattern of global mantle flow, which evolves on a much longer time scale on the order of 150-200 m.y. [Bunge et al., 1998], they must reflect temporal variations in plate coupling along a given margin. A prominent example is the 30% slowing of convergence between the Nazca and South America plates over the past 10 m.y. (fig. 1) inferred from a variety of data [Norabuena et al., 1999]. We propose that the slowing of convergence results from the mechanism causing pronounced along-strike trench-parallel gravity anomalies (TPGAs) (fig 2a). We compute these anomalies by subtracting the regional-average trench-normal gravity profile from free-air gravity data [Sandwell and Smith, 1997]. The TPGA profile along the Nazca/South America margin is characterized by strongly negative values, as large as -100 mGal, in the central part close to the highly elevated Puna and Altiplano regions. In contrast, the northern and southern parts of the trench show both a positive signal. TPGA gradients coincide with the occurrence of large earthquakes - such as the great M 9.5 Chilean event of 1960 [Barrientos and Ward, 1990] and the recent M 8.0 Peru earthquake of 2007 - and are associated with substantial trench parallel bathymetry variations [Smith and Sandwell, 1997]. It has been suggested that the largest earthquakes occur on portions of subduction zones where plates are most strongly coupled [Kanamori, 1986], thus TPGAs might be indicative of lateral variations in mechanical coupling [Stein and Wysession, 2003]

63

along the plate margin. One way to estimate plate coupling is from computer simulations using global models of the lithosphere that include sophisticated rheologies and realistic plate configurations [Bird, 1999]. The stresses involved in the dynamics of the lithosphere include the tectonic contribution coming from regions of high topography, which provide both horizontal deviatoric stresses and vertical overburden pressure, and the shear stresses from buoyancies in the mantle. Typically these models reduce the computational complexity of the dynamic system by exploiting isostasy and vertical integration of stresses in the so-called thin-shell approximation, with a shortcoming arising from the need to parameterize mantle buoyancy and flow generating shear stresses at the base of plates. At the same time there has been great progress in our ability to simulate the circulation of Earth's mantle at high numerical resolution [Bunge et al., 1997]. Such time-dependent earth models account for radial variations in mantle viscosity (typically a factor 40 increase from the upper to the lower mantle), internal heat generation from radioactivity, bottom heating from the core, and a history of subduction spanning the past 120 m.y., and provide a first-order estimate of internal mantle buoyancy forces that drive plates; the models, however, do not account for the brittle nature of the faulted lithosphere and, specifically, for the contribution of plate boundary forces to the stress balance. It is logical therefore to merge these two independent classes of models. Using the global model for lithosphere dynamics SHELLS [Kong and Bird, 1995] combined with 3D

mantle circulation models [Bunge et al., 2002] we have shown recently that late Miocene/Pliocene uplift of the Andes can account for the rapid Nazca/South America convergence reduction over the past 10 m.y. [Iaffaldano et al., 2006].

MODELS AND RESULTS

Global coupled lithosphere/mantle circulation models allow us to derive an explicit budget of plate boundary forces along the Nazca/South America plate margin. Under the assumption that plate boundary forces along the margin are dominated by the recent uplift of the Andes, we use the SHELLS global model accounting for the present-day topography as reported in the ETOPO5 data set [National Geophysical Data Center, 1998] and shear tractions taken from the above-mentioned simulations of mantle flow, to compute equilibrium forces in the lithosphere. We then perform a second simulation corresponding to a paleoreconstruction of topography of the Andes 10 m.y. ago [Gregory-Wodzicki, 2000]. The plate boundary forces along the Nazca/South America margin that correspond to the recent uplift of the Andes are obtained as the difference of the two simulations. It is worth mentioning that among others, one advantage of such approach is that it allows neglecting with reasonable confidence viscous deformation within the Andean belt, since its growth is included in

65

our simulations not as a time-evolving process but rather as initial and final stages. We find that the average resisting force upon the Nazca plate from gravitational spreading of the Andes is on the order of $3.7*10**12$ N/m, a value comparable to results from previous 2D studies [Husson and Ricard, 2004]. Integrated over the total length of the plate boundary (5300 Km) the net average force equals $2*10**19$ N. More interesting is the along-strike variation of the Andean-related plate boundary forces. For ease of comparison we treat the plate boundary forces due to Andean uplift in the same manner as the trench parallel gravity anomalies. That is, we subtract the average resisting force along the margin from the local plate boundary forces in our simulations. Along the central portion of the margin we find strongly positive force anomalies, as high as $3*10**12$ N/m, whereas negative anomalies prevail in the northern and southern parts. Figures 2a and 2b reveal a remarkable correlation of TPGAs and plate boundary forces predicted from Miocene/Pliocene uplift of the Andes in our model. The gravity signal shows pronounced short wavelength spatial variations from positive to negative values suggestive of a shallow origin of the associated mass anomalies. Our predicted trench-parallel resisting forces anomalies display a similar behavior. Gravity and resisting force anomalies along the trench are highly correlated at the 90% confidence level (fig. 2c). In fig. 3a we plot the observed trench parallel bathymetry anomalies obtained by subtracting the average trench-parallel bathymetric profile from the digital elevation model ETOPO5. The trench-

parallel gravity (fig. 2a) and bathymetry (fig. 3a) anomalies are in excellent agreement, an inference suggested earlier by Song and Simons [2003]: negative gravity anomalies correspond to deeper than average bathymetry whereas positive anomalies correspond to bathymetry shallower than the average. We note that the age of the Nazca ocean floor varies between 20 and 50 m.y. along the margin [Müller et al., 1997], and that a simple half-space model of plate subsidence due to lithosphere cooling would predict ocean depth variation of about 1 Km, accounting for only 25% of the observed bathymetric variations. We test whether the magnitude of plate coupling forces arising from our simulations is sufficient to explain the observed bathymetry signal by solving for an analytical solution of the thin-plate differential equation for a semi-infinite oceanic plate, tectonically loaded on one side (see inset in fig. 2b). A Young modulus of 20 GPa, Poisson ratio of 0.25, and an elastic thickness in the range 25 - 30 Km are assumed, consistent with published estimates [Caldwell et al, 1976]. We take the analytical solution to compute vertical bending of the Nazca plate under the action of our predicted force anomalies. We also account for gravitational restoring forces from the denser asthenosphere, as well as for intrinsic bathymetric variations related to the cooling of oceanic lithosphere. Predicted bathymetry anomalies are shown in fig. 3b. We map the lack and excess of mass expressed by computed bathymetry anomalies into predicted gravity anomalies by integrating a Bouguer gravity formula for water against crust along the computed bathymetric anomaly profile of Nazca plate. Our

predictions of the gravity signal are in excellent agreement with the observations (fig. 3c).

DISCUSSION

Our results raise an important question: Could there be other mechanisms capable of providing a simultaneous explanation for the observed slowing of convergence over the past 10 m.y. and the pronounced gravity and bathymetry signals along the margin? For instance, the amount of sea-floor sediments varies substantially along the trench [Mooney et al., 1998]. Sediment thickness in the northern and southern part of the margin is higher than 1500 m whereas the central part, between 13°S and 30°S, is sediment-starved. It has been suggested that lack of sediment infill may be responsible for stronger plate coupling by increasing the effective coefficient of friction along the central sediment-starved portion of the trench [Lamb and Davies, 2003]. This would result in higher resisting stresses in these regions [Kohlstedt et al., 1995], which would oppose convergent motion. We test this hypothesis in fig. 4. Because we lack a direct relationship between the amount of sediment infill and the friction coefficient, we compute plate coupling and associated convergence velocity for a range of friction coefficients in the sediment-starved part of the trench. Specifically, we compute and

then subtract from each other two equilibrium force-fields: one is associated with homogeneous friction along the trench, the other features increased friction in the sediment-starved portion of the trench between 13°S and 30°S. Our results show that the convergence velocity is rather insensitive to the assumed friction coefficient, and that one requires a friction value as high as 0.4 to result in a convergence reduction compatible with observations (shown in green in fig. 4). Such high value, however, is close to the prediction from Byerlee's law for failure of materials (shown in blue) and much larger than the commonly accepted limit for convergent margins of 0.1 (shown in red). Theoretical 2D studies of the Andean orogeny [Sobolev and Babeyko, 2005] reveal in fact that friction coefficients higher than 0.1 would produce slab break-off, thus stopping the subduction process. From this we conclude that frictional variations along the Nazca/South America plate margin are unlikely to provide a simultaneous explanation for the observed convergence record, the bathymetry anomalies and the TPGAs along the Nazca/South America plate boundary. Instead these observations are best explained by large topographic features, such as the high plateaus in the central Andes. We speculate, however, that friction-generated variations in trench-parallel plate boundary forces might explain moderate TPGAs in other regions of plate convergence where high topography is not a dominant feature. Our results suggest that variations of mechanical coupling along the plate boundary are the origin for the peculiar shape of the South American margin, with its strong indentation near the Puna

and Altiplano plateaus. Paleomagnetic evidence indicates that rotation in the Bolivian orocline occurred over the past 7 to 9 m.y. [Rousse et al., 2003]. The timing is significant in that it is coeval with the most recent uplift of the Andes. The variations in plate boundary forces inferred from our models are consistent with recent along-strike variations in shortening rates [Hindle et al., 2002] and imply large torques that may have contributed to the present-day convex profile in a feedback process between plate convergence and mountain belt growth. Our inference represents an alternative to an earlier finding by Russo and Silver [1994]. Based on observations of seismic anisotropy beneath the Nazca/South America trench, they suggested that mantle stagnation under the central margin and corner flow in the northern and southern edges resulted in increased shortening in the central Andes, an inference that Isacks [1988] proposed as possible origin for the curvature of the trench. In a recent paper Schellart et al. [2007] used numerical cartesian models for the dynamics of a subducting viscous slab with no overriding plate to test whether mantle flow could be generated in the first place by the tendency of a wide trench to roll back at its edges. Although they find that such process may occur, they observe that it would take some 50 m.y. to develop. The main difficulty with this view would then be to explain why the convexity developed only recently [Allmendinger et al., 2005], as subduction has been active off-shore of South America for at least the past 200 m.y. [Allmendinger et al., 1997]. Our results are interesting in that they suggest that observations and modeling tools have reached a

level of maturity where it is possible to identify a range of plate boundary forces, including those arising from gravitational spreading of large topographic features. They also suggest that coupled lithosphere/mantle models can now be used to make specific predictions about their spatial and temporal distribution along a given margin. Because plate margin forces are a key-controlling element in how plates move, our results imply that the understanding of the dynamic processes in plate tectonics can be advanced.

REFERENCES

Allmendinger, R. W., Jordan, T. E, Kay, S. M., and Isacks, B. L., 1997, The evolution of the Altiplano-Puna plateaus of the central Andes: Annual Review of Earth and Planetary Science, v. 25, p. 139-174.

Allmendinger, R. W., Smalley, R. Jr., Bevis, M., Caprio, H. and Brooks, B., 2005, Bending the Bolivian orocline in real time: Geology, v. 33, p. 905-908.

Barrientos, S. E. and Ward, S. N., 1990, The 1960 Chile earthquake – Inversion for slip distribution from surface deformation: Geophysical Journal International, v. 103, p. 589-598.

Bird, P., 1999, Thin-plate and thin-shell finite element programs for forward dynamic modeling of plate deformation and faulting: Computers & Geosciences, v. 25, p. 383-394.

Bunge, H.-P., Richards, M.A. , and Baumgardner, J.R., 1997, A sensitivity study of three-dimensional spherical mantle convection at 10exp8 Rayleigh number: Effects of

depth dependent viscosity, heating mode and an endothermic phase change: Journal of Geophysical Research, v. 102, p. 11991-12007.

Bunge, H.-P., Richards, M. A. and Baumgardner, J. R., 2002, Mantle-circulation models with sequential data assimilation: Inferring present-day mantle structure from plate-motion histories: Royal Society of London Philosophical Transaction Ser. A., v. 360, p. 2545-2567.

Bunge, H.-P., Richards, M. A., Lithgow-Bertelloni, C., Baumgardner, J. R., Grand, S. P. and Romanowicz, B. A., 1998, Time scales and heterogeneous structures in geodynamic earth models: Science, v. 280, p. 91-95.

Caldwell, J. G., Haxby, W. F., Karig, D. E. and Turcotte, D. L., 1976, On the applicability of a universal elastic trench profile: Earth and Planetary Science Letters, v. 31, p. 239-246.

Data Announcement 88-MGG-02, Digital relief of the Surface of the Earth. NOAA, National Geophysical Data Center, Boulder, Colorado, 1988.

DeMets, C., Gordon, R. G., Argus, D. F. and Stein, S., 1994, Effect of recent revisions to the geomagnetic reversal time scale on estimates of current plate motions: Geophysical Research Letters, v. 21, p. 2191-2194.

Dixon, T. H., 1991, An introduction to the Global Positioning System and some geological applications: Review of Geophysics, v. 29, p. 249-271.

Forsyth, D. W. and Uyeda, S., 1975, Relative importance of driving forces of plate motion: Geophysical Journal of the Royal Astronomical Society, v. 43, p. 163-200.

Gregory-Wodzicki, K. M., 2000, Uplift history of the central and northern Andes: A review: Geological Society of America Bulletin, v. 112, p. 1091–1105.

Hindle, D., Kley, J., Klosko, E., Stein, S, Dixon, T. and Norabuena, E., 2002, Consistency of geologic and geodetic displacements during Andean orogenesis: Geophysical Research Letters, v. 29, p. 1188 - 1192.

Husson, L. and Ricard, Y., 2004, Stress balance above subduction: application to the Andes: Earth and Planetary Science Letters, v. 222, p. 1037-1050.

Iaffaldano, G., Bunge, H.-P. and Dixon, T. H., 2006, Feedback between mountain belt growth and plate convergence: Geology, v. 34, p. 893-896.

Isacks, B. L., 1988, Uplift of the central Andean plateau and bending of the Bolivian Orocline: Journal of Geophysical Research, v. 93, p. 3211-3231.

Kanamori, H., 1986, Rupture process of subduction-zone earthquakes: Annual Review of Earth and Planetary Science, v. 14, p. 293-322.

Kohlstedt, D. L., Evans, B. and Mackwell, S. J., 1995, Strength of the lithosphere: Constraints imposed by laboratory experiments: Journal of Geophysical Research, v. 100, p. 17,587-17,602.

Kong, X. and Bird, P., 1995, SHELLS: A thin-shell program for modeling neotectonics of regional or global lithosphere with faults: Journal of Geophysical Research, v. 100, p. 22,129-22,131.

Lamb, S. and Davies, P., 2003, Cenozoic climate change as a possible cause for the rise of the Andes: Nature, v. 425, p. 792-797.

Mooney, W. D., Laske, G. and Masters, T. G., 1998, CRUST 5.1: a global crustal model at 5 x 5 degrees: Journal of Geophysical Research, v. 103, p. 727-748.

Morgan, W. J., 1968, Rises, trenches, great faults, and crustal blocks: Journal of Geophysical Research, v. 73, p. 1959-1982.

Müller, R.D., Roest, W.R., Royer, J.-Y., Gahagan, L.M. and Sclater, J.G., 1997, Digital isochrons of the world's ocean floor: Journal of Geophysical Research, v. 102, p. 3211-3214.

Müller, R. D., Sdrolias, M., Gaina, C. and Roest, W. R., 2008, Age, spreading rates and spreading asymmetry of the world's ocean crust: in press on Geochemistry Geophysics and Geosystems.

Norabuena, E. O., Dixon, T. H. STEIN, S., and HARRISON, C. G. A., 1999, Decelerating Nazca-South America and Nazca-Pacific plate motions: Geophysical Research Letters, v. 26, p. 3405-3408.

Ricard, Y. and Vigny, C., 1989, Mantle dynamics with induced plate tectonics: Journal of Geophysical Research, v. 94, p. 17543-17559.

Rousse, S., Gilder, S., Farber, D., McNulty, B., Patriat, P., Torres, V. and Sempere, T., 2003, Paleomagnetic tracking of mountain building in the Peruvian Andes since 10 Ma.: Tectonics, v. 22, p. 1048-1069.

Russo, R. M., and Silver, P. G., 1994, Trench-parallel flow beneath the Nazca plate from seismic anisotropy: Science, v. 263, p. 1105-1111.

Sandwell, D. T. and Smith, W. H. F., 1997, Marine gravity anomalies from Geosat and ERS 1 satellite altimetry: Journal of Geophysical Research, v. 102, p. 10039-10054.

Schellart, W. P., Freeman, J., Stegman, D. R., Moresi, L. and May, D., 2007, Evolution and diversity of subduction zones controlled by slab width: Nature, v. 446, p. 308-311.

Smith, W. H. F. and Sandwell, D. T., 1997, Global sea floor topography from satellite altimetry and ship depth soundings: Science, v. 277, p. 1956-1962.

Sobolev, S. V. and Babeyko, A. Y., 2005, What drives orogeny in the Andes?: Geology, v. 33, p. 617-620.

Song, T. R. A. and Simons, M., 2003, Large trench-parallel gravity variations predict seismogenic behavior in subduction zones: Science, v. 301, p. 630-633.

Stein, S., 1993, Space geodesy and plate motions: Contributions of space geodesy to Geodynamics, p. 5-20.

Stein, S. and Wysession, M., 2003, Introduction to Seismology, Earthquakes and Earth Structure: Blackwell Publishing, p. 323.

Past (red) and present (blue) motions of NZ and SA plates
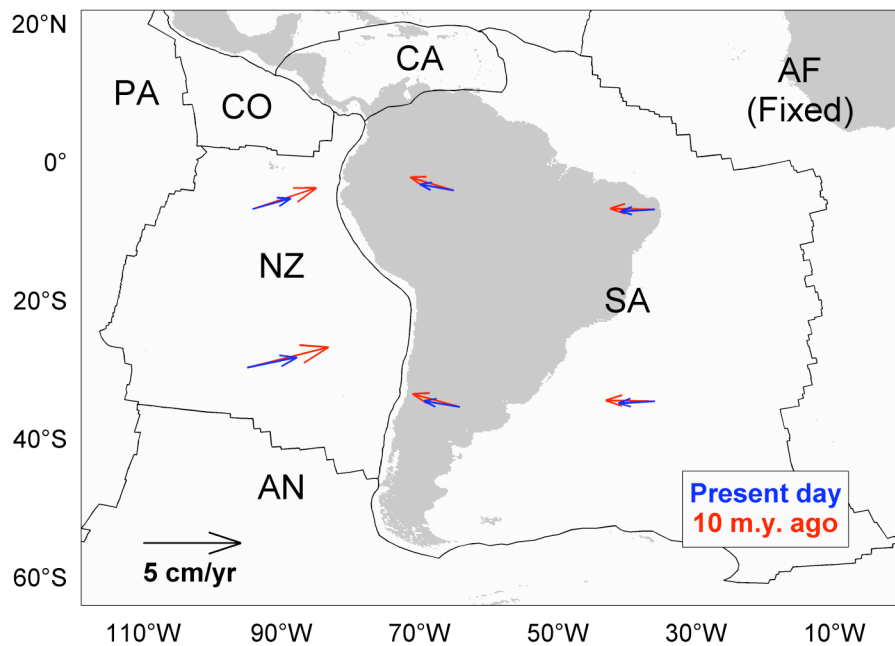
Fig. 3.1. Comparison of past (10 m.y.) and present-day motion of Nazca (NZ) and South America (SA), derived from paleomagnetic (red) and instantaneous geodetic observations (blue). Velocity vectors reveal a 30% convergence reduction from 10 to 7 cm/yr over the past 10 m.y. The timing suggests a co-evolution of increased plate coupling forces and Andean uplift. Plate boundaries are in black, continents are in gray. Plate abbreviations: AF-Africa, AN-Antarctica, CA-Carribean, CO-Cocos, PA-Pacific.
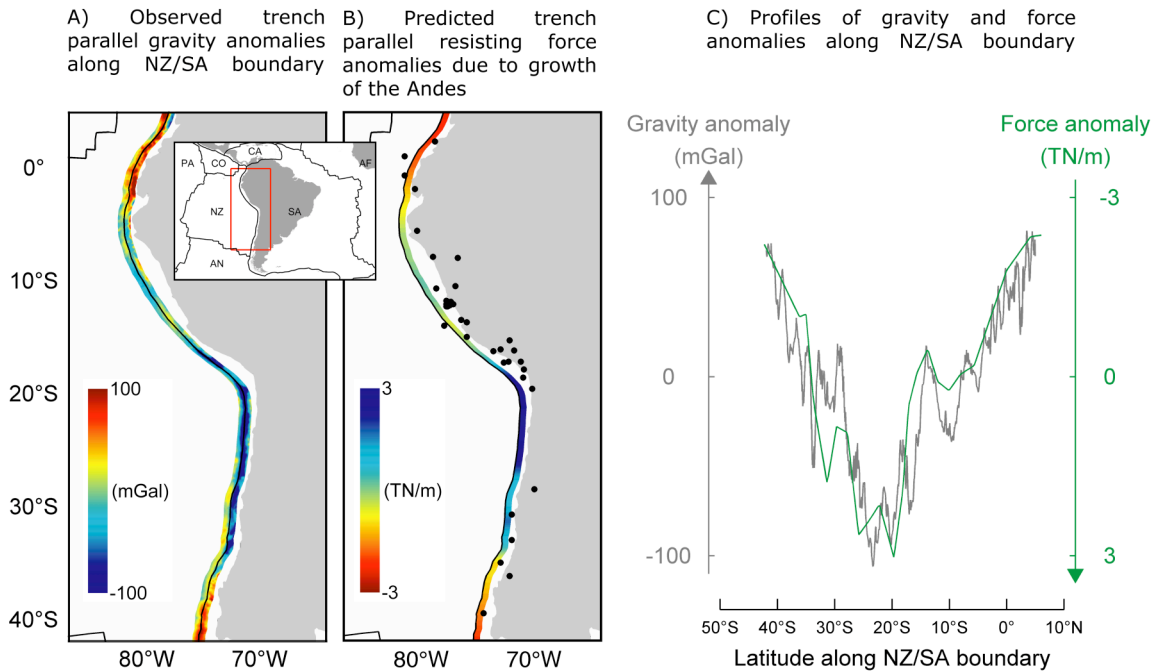
Fig. 3.2. (a) Observed TPGAs along the Nazca/South America plate margin (see text). Anomalies as high as +/- 100 mGal vary rapidly from north to south along the margin, and suggest a shallow origin of the gravity signal. **(b)** Predicted tectonic force anomalies due to rise of the Andes (see text for details). Force anomalies are obtained by subtracting the average resisting force along the margin from the local plate boundary forces in our simulations. Note the strongly positive force anomalies, as high as 3*10**12 N/m, along the central portion of the margin whereas negative anomalies prevail in the northern and southern parts. Black dots indicate large (Mw > 8.0)

earthquakes reported since 1555, which occurred in regions of moderate to low coupling between subducting and overriding plates. **(c)** Comparison of the along-trench profile of gravity and tectonic force anomalies. The two profiles correlate at 90% confidence level.

a) Observed trench parallel bathymetry anomalies along NZ/SA boundary

b) Predicted trench parallel bathymetry anomalies along NZ/SA boundary

c) Predicted and Observed trench parallel gravity anomalies along NZ/SA boundary
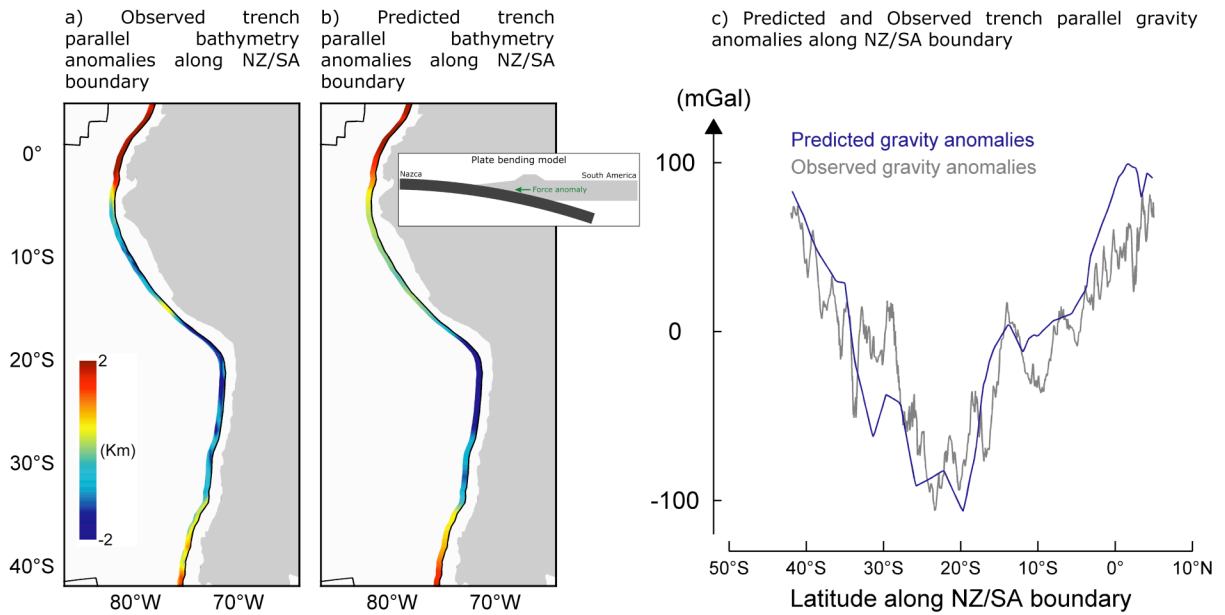
Fig. 3.3. Trench parallel bathymetry anomalies observed **(a)** and predicted **(b)** from an analytical plate-bending model (see text and inset) using the tectonic forcing computed from our models. Predicted magnitude and spatial pattern of the bathymetry anomalies are in excellent agreement with observations. **(c)** Observed (grey) and predicted (blue) gravity anomaly profiles along the Nazca/South America plate boundary. Predicted gravity anomalies are computed by integrating a Bouguer formula for density of water against crust along bathymetry-anomaly profiles predicted from our simulations. The two profiles correlate at the 90% confidence level and confirm that gravity anomalies and plate coupling variations along the convergent margin are associated with recent growth of the Andes (see text).
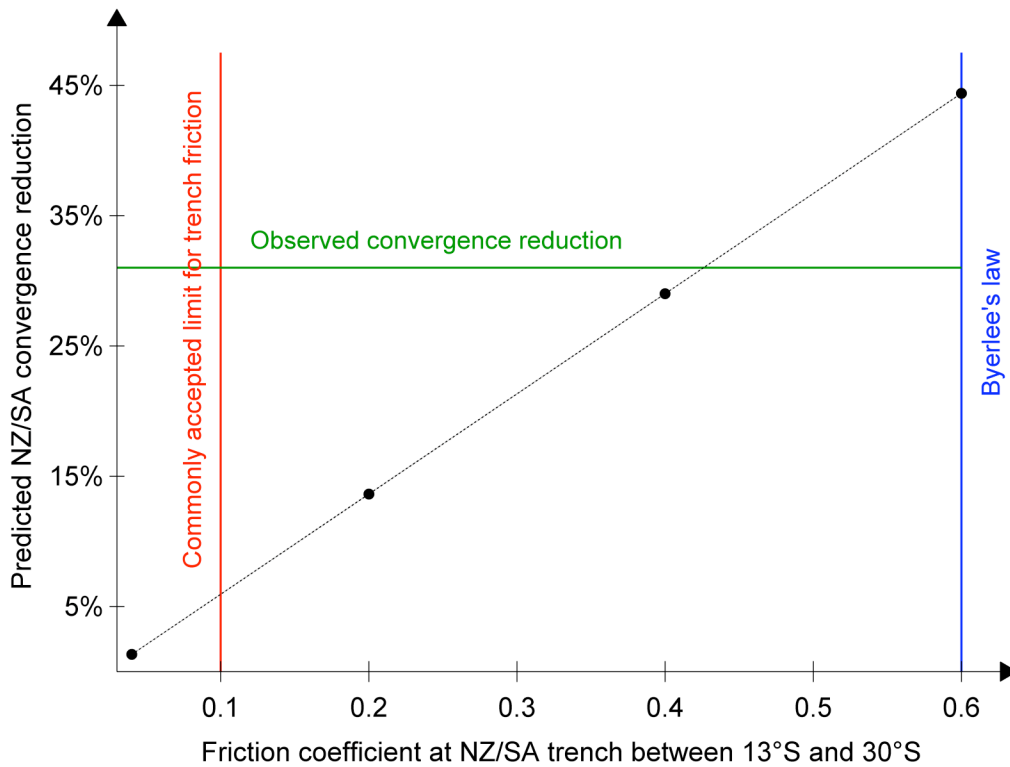
Fig. 3.4. Predicted Nazca/South America (NZ/SA) convergence reduction for a range of assumed friction coefficients along the sediment-starved plate boundary, between 13°S and 30°S. Friction values smaller than 0.1, which is a commonly accepted limit for trench friction (see red line), cannot explain the observed convergence reduction (see green line). To explain the observed 30% velocity reduction through frictional variations along the sediment-starved portion of the margin it requires high friction values, close to 0.6 (see blue line - Byerlee's law for failure of materials under stresses larger than 200 MPa).

Conclusions

In this thesis I prove the potential and the effectiveness of such joint approach by predicting various, seemingly unrelated observables at the convergent boundary between Nazca and South America plates. I compute a detailed force budget along the Nazca/South America subduction zone, showing that a large portion of it comes from the recent uplift of the Andes. Results show that forces computed with the global, coupled models provide simultaneous explanations for (1) trench parallel gravity anomalies, (2) pronounced bathymetry variations, as well as (3) a substantial reduction in Nazca/South America plate convergence recorded over the past 10 million years. All these observations can be explained from along-trench, lateral and temporal variations in plate coupling forces that are predicted from my simulations.

Results demonstrate that surface topography generated at convergent margins is a key factor controlling the evolution of plate tectonics. Specifically, the topographic load of large mountain belts and plateaus consumes a significant amount of the force available by increasing resisting forces between downgoing and overriding plates.

Lebenslauf

Persönliche Daten

Name   Giampiero Iaffaldano

Anschrift   Nymphenburgerstrasse 106, 80636 München

Geburstdatum   14 November 1978

Geburstort   Bari – Italien

Schulausbildung

1985 – 1993 Grundschule, Rutigliano – Italien

1993 – 1997 Gymnasium, Rutigliano – Italien

Hochschulausbildung

1998 – 2003 Master (Physik) Universita' degli studi di Roma "La Sapienza", Roma –

Italien